Testing for Asset Price Bubbles using Options Data*

Nicola Fusari† Robert Jarrow ‡ Sujan Lamichhane§

First Version: August 2020
Updated: May 2022

Abstract

We present a new approach to identifying asset price bubbles based on options data. We estimate asset bubbles by exploiting the differential pricing between put and call options. We apply our methodology to two stock market indexes, the S&P 500 and the Nasdaq-100, and two technology stocks, Amazon and Facebook, over the 2014-2018 sample period. We find that, while indexes do not exhibit significant bubbles, Amazon and Facebook show frequent and significant bubbles. The estimated bubbles tend to be associated with large volatility, large trading volume, and earning announcement days. Since our approach can be implemented in real time, it is useful to both policy-makers and investors. As an illustration we consider two case studies: the Nasdaq dot-com bubble (between 1999 to 2002) and GameStop (between December 2020 and January 2021). In both cases we identify significant and persistent bubbles.

Keywords: Asset Price Bubbles, Option Pricing, Stochastic Volatility, Martingales, Local Martingales.
JEL classification: C51, C52, G12, G13.

*We thank Torben Andersen, Maria Teresa Gonzalez-Perez (MFA discussant), Kris Jacobs, Igor Makarov (AFA discussant), Dimitris Papadimitriou (EFA discussant), Nagpurnanand Prabhala, Eric Renault, Olivier Scaillet, and Viktor Todorov for their comments and suggestions, as well as seminar participants at Dhuram University, 2021 MFA conference, 2021 Vienna Workshop on the Econometrics of Options Markets, 2021 EFA conference, and 2022 AFA conference.

†Johns Hopkins Carey Business School, Baltimore, M.D. 21202, email: nfusari1@jhu.edu.

‡S.C. Johnson Graduate School of Management, Cornell University, Ithaca, N.Y. 14853 and Kamakura Corporation, Honolulu, Hawaii 96815, email: raj15@cornell.edu.

§International Monetary Fund, email: sl2563@cornell.edu. The views expressed in this paper are those of the authors and do not necessarily represent the views of the IMF, its Executive Board, or IMF management.

1 Introduction

Price bubbles arise because buyers often purchase an asset not to hold it forever and capture its perpetual cash flows but to resell it at a higher price sometime in the future. The existence of a bubble is therefore closely related to investors' expectations about the future evolution of the asset price. Thus, options, with their forward-looking nature, are the natural instruments to estimate and test for the existence of bubbles in their underlying assets. In this paper we develop (i) an easy-to-implement *estimation* procedure that enables us to quantify the magnitude of a price bubble, and (ii) a *statistical test* that we use to assess the significance of the estimated price bubble. Importantly, option prices are the only input required to carry out the estimation. Increased liquidity on the option market over the last decade, along with an ever-increasing number of options traded and quoted over a large range of strikes,[1] facilitates the effective and reliable implementation of our methodology.

Our methodology builds on the fact that traded call and put options reflect price bubbles differently (see Section 2.1 below). This insight is an implication of the local martingale theory of bubbles, as developed in Loewenstein and Willard (2000b), Loewenstein and Willard (2000a), Cox and Hobson (2005), Heston et al. (2007), and Jarrow et al. (2010). This theory assumes markets are arbitrage-free and defines a price bubble to be the difference between the market price of an asset S_t and its fundamental value S_t^*, i.e. the asset's expected discounted cash flows using a risk neutral measure. A bubble arises when the (discounted) price process is a supermartingale, and not a martingale under the risk neutral measure. In this case, while the standard risk neutral (RN) valuation methodology can be shown to apply to put options (i.e. the market prices of a put option P_t corresponds to its RN value P_t^*), RN valuation does not apply to the price of a call option because a call option's price may contain a bubble. Consequently, its market price C_t can deviate from its RN valuation C_t^*. Furthermore, if the market is also assumed to satisfy no-dominance, or equivalently put-call parity holds, then the option's bubble $(C_t - C_t^*) \geq 0)$ is linearly related to the price bubble $(S_t - S_t^*)$ in the underlying asset.[2] Although the call option's bubble vanishes as the option matures, a call option's bubble provides a lower bound for the size of the bubble in the underlying asset. Of course, the underlying asset's bubble is independent of the option's maturity. It is this last linear relation that enables us to test for the existence of an underlying's price bubble using just option prices.

Figure 1 illustrates these option price relations for the Nasdaq index on January 2, 2001

[1] As shown, for example, by Andersen et al. (2017) for the case of the SP&P 500 index.
[2] See Section 2 for the definition of no-dominance.

for an option cross-section with 17 days-to-maturity. The figure plots the corresponding Black and Scholes implied volatilities for ease of presentation.[3] The left panel shows the observed market (green triangles) implied volatilities versus the model-implied risk-neutral ones for put options (i.e. the implied volatility computed using the put's fundamental value). As seen, the two lines, even if the market data is affected by some degree of noise, greatly overlap, pointing to the equality between the market and fundamental values of put options (i.e., $P_t = P_t^*$). In contrast, the right panel shows a different situation for the call options. We see that there is a consistent positive gap between the market price of call options (green triangles) and their fundamental values (i.e., $C_t > C_t^*$).[4]

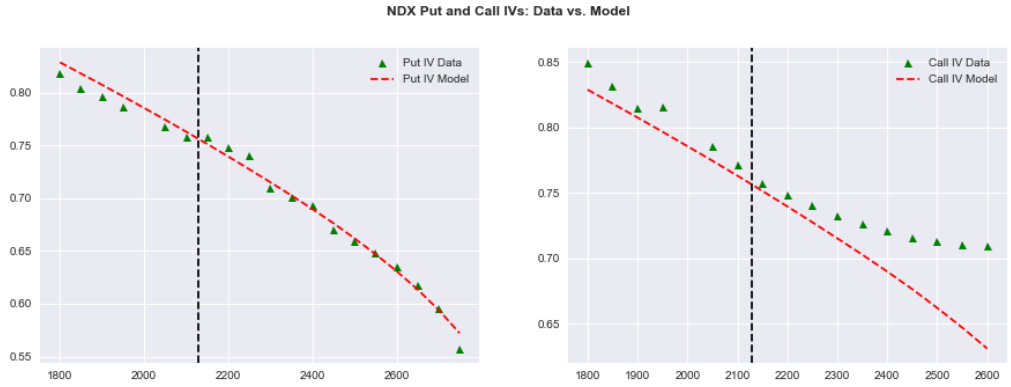

Figure 1: **Puts, Calls, and Bubble**: The figure reports the estimation results for Nasdaq on January 2, 2001 (17 days-to-maturity option cross-section). The figure shows in the left (right) panels, the observed implied volatility of put (call) options, green triangles, and the implied volatility computed using puts (calls) fundamental values, red dashed line.

This positive gap identifies a positive call option bubble. The importance of being able to identify a call option bubble is twofold. First, from a theoretical point of view, it can be shown that whenever ND holds in the market, or equivalently, put-call parity is not violated, the call option bubble reflects a bubble in the underlying asset. In this case, a bubble in the underlying asset can be identified by simply looking at real-time option data, without the need to use past time-series data. It is important to note, however, that the existence of a call option's bubble is independent of whether or not put-call parity holds. A violation of put-call parity only weakens the linear relation between the call option's bubble and the

[3]We do not use the Black and Scholes (1973) model to price the options. The Black and Scholes model simply provides a quoting device to transform prices into implied volatilities, because there is a 1-1 relation between prices and implied volatilities.

[4]The details on how we compute the fundamental value of put and call options are described in Section 2.

underlying stock's price bubble.[5]

Second, there is a recent strand of the literature that studies options as financial assets in and of themselves, studying option return characteristics (e.g. Goyal and Saretto (2009), Cao and Han (2013), and more recently Büchner and Kelly (2022)), their return predictability (e.g. Zhan et al. (2021) and references therein), their factor structure (see Christoffersen et al. (2018)), and to compute bounds on expected returns using option prices (both puts and calls, see Chabi-Yo et al. (2021)). Even when ND does not hold, our methodology is still able to identify and quantify bubbles in call options, which is relevant to the above research.

We develop a three-step procedure to estimate a bubble in the asset price. First, we propose a flexible parametric model for the evolution of the asset's price process. The model, for different values of its parameters, needs to admit both a martingale and a strict local martingale representation. This requirement stems from the fact that, as shown in Jarrow et al. (2010), a process admits a price bubble if and only if it is a strict local martingale. We use the family of processes posited in Andersen and Piterbarg (2007). To address model misspecification concerns, we augment this class of models with price jumps in order to better fit option prices. We call the resulting model the generalized stochastic volatility jump diffusion (G-SVJD) model. The G-SVJD model subsumes many of the models commonly used in the option-pricing literature, such as the Merton (1976), the Heston (1993) stochastic volatility, and the Bates (1996) stochastic volatility with jump model. Second, we estimate the G-SVJD model using *only* put options[6] because, as noted above, put options do not exhibit bubbles and standard risk neutral valuation applies. Thus, in this step the G-SVJD model is both estimated and tested for accuracy on put options. Third, we use the estimated G-SVJD to compute a call option's bubble, which is the difference between the call's market price and its risk neutral value. When put-call parity holds, this difference is linearly related to the underlying asset's price bubble and provides a lower bound.

Finally, we develop a statistical test to assess the significance of the estimated call option bubble which takes into account potential model misspecification and measurement errors.[7] If the call option bubble is significant, positive, and ND holds, then the underlying asset's price bubble is significantly different from zero as well (and arguably much larger). Because our approach can be implemented in real time, it is useful for both policy-makers and in-

[5]See Section 3.4 for details on how we deal with potential violation of put-call parity, early exercise premium in the case of American options, and other market frictions.

[6]We use both in-the-money and out-of-the-money put options in this step in order to span the entire support of the risk neutral distribution.

[7]Figure 1 exemplifies the extent of measurement error in option implied volatilities and, in turn, in option prices.

vestors who need a forward-looking approach for daily monitoring of the financial system for effective risk management.[8]

We apply our methodology to four assets over the 2014-2018 period: the S&P 500 (SPX) and the Nasdaq-100 (NDX) – two indexes that represent broad market movements – and Amazon (AMZN) and Facebook (FB) – two popular technology stocks. Our analysis reveals that SPX and NDX do not show episodes of price bubbles.[9] In sharp contrast, both AMZN and FB exhibit many more instances of large and persistent positive bubbles.

Our results challenge the widespread tendency to label periods marked by rapidly rising stock prices as representing bubbles. For example, from 2016 to mid-2018, FB's price increased from around \$100 to over \$200, exceeding a 100% price increase. Similarly, AMZN rose from \$500 in early 2016 to around \$1200 by late 2017, exceeding a 140% increase. However, we did not find any significant call option bubbles during these periods. From a theoretical point of view (see Section 2 for details) a asset price bubble exists when volatility rises faster than the price itself. As higher asset volatility is usually associated with a higher level of buying/selling, this can be interpreted as representing an economic motive to capture the future resale value. We provide evidence of this fact by showing that bubbles tend to be associated with periods of increased volatility (as measured by the risk-neutral quadratic variation) and increased trading activity. Furthermore, we show that the probability of a bubble increases in the period preceding earnings announcements.

We then study the relation between our parameter estimates for the underlying asset's price process and the option-based bubble estimates. Even if our empirical methodology estimates the option's fundamental value with very high accuracy, some parameters are estimated with large standard errors because they tend to have similar impact on the asset's price distribution. This is analogous to a linear regression with a large R^2, but where the independent variables are highly correlated (a multicollinearity problem). As previously noted, our theory imposes strict conditions on the parameter values that are compatible with an underlying asset's price bubble. Studying these parameters, despite their large standard errors, we find a significant link between the estimated model's parameters and the identified call option bubbles. In particular, we show that the estimated parameters help explain both the magnitude and the probability of the stock price bubbles, providing both an indirect test of the satisfaction of put-call parity, and the validity of our option based

[8]This is especially true because our approach can be applied to options data on equity indexes, individual stocks, and also ETFs.

[9]We measure the magnitude of the option's bubble as a percentage of the underlying asset's price. See section 3.3 for more details.

methodology for identifying stock bubbles.

Finally, to illustrate that our methodology can detect stock price bubbles during periods widely perceived as exhibiting bubbles, we consider the Nasdaq (NDX) dot-com bubble in the early 2000s and the more recent meteoric rise of GameStop (GME). We show that our call option based approach detects large and persistent stock price bubbles during the dot-com boom of early 2000. For GME, we detect a bubble starting in December 2020 that remains large in magnitude and significant throughout January. These results are consistent with the short-run rise (and consequent fall) of GME's stock price between January and February 2021. Both the dot-com bubble and the GME case studies further provide empirical support for our proposed approach.

Discussion: Before we present our analysis, we consider the economics underlying the existence of bubbles. Given investors' heterogeneous beliefs, bubbles arise because buyers purchase an asset, not necessarily to hold it forever, but to resell it at a premium sometime in the future. This idea can be traced back to Harrison and Kreps (1978) and has been discussed recently in Scheinkman (2013), Xiong (2013), and Jarrow (2015). We can conceive of a risky asset's fundamental value as the price an investor would pay for holding the asset until its maturity, i.e. purely a buy-and-hold value. A price bubble reflects the idea that the resale value, the market price, exceeds the buy-and-hold value.[10] Thus, a price bubble is not an absolute concept, but rather a relative one with respect to some fundamental value (which may be unobservable). Intuitively, a bubble exists when the motive to buy an asset is not to hold it forever and consume the asset's cash flows (i.e. dividends) but rather to resell the asset at some (potentially random) future time for a (potentially) higher price.[11] As a consequence, one might expect that the stronger the reselling motive, the larger the bubble magnitude.

Related Literature: There is a related strand of the econometrics literature that develops estimators of price bubbles using historical time-series asset prices and alternative methods (e.g. see Phillips et al. (2015a), Phillips et al. (2015b), and Phillips and Shi (2018))[12]. These

[10] A concrete example is the amount one is willing to pay to buy a work of art if after the purchase it must be held forever (and cannot be resold) – this is the fundamental value. The market price is the amount one is willing to pay if there is a possibility of selling the art at a higher price sometime in the future.

[11] In fact, we rarely see investors hold onto an asset forever and never liquidate it. Even the most notable long-term investor, Warren Buffett, periodically liquidates existing stock positions and/or adds new positions with holding periods longer than for most other investors, but nevertheless the holding periods are still finite. For a more detailed discussion of this view, see Jarrow (2016).

[12] Also see Giglio et al. (2016) for an empirical analysis of the existence of housing bubbles in the United Kingdom and Singapore.

papers use a different model structure and a different definition of an asset price bubble. Our model has continuous trading over a finite horizon; theirs features discrete trading over an infinite horizon. The distinction between discrete and continuous trading is important because in discrete time there are only two types of asset price bubbles possible, while in continuous time there are three.

Indeed, as discussed in Jarrow et al. (2010) and Jarrow (2015), in continuous time models there are three types of bubbles, called type 1, type 2, and type 3. A type 1 bubble exists only in infinite horizon models, and it captures fiat money (a security with zero cash flows but strictly positive value). These bubbles typically don't exist in frictionless market asset pricing models that don't include cash. A type 2 bubble also exists only in infinite horizon models and it corresponds to an asset whose price process (under the risk neutral probability) is a martingale but not a uniformly integrable martingale. Intuitively, the risk-adjusted expected discounted cash flows and liquidation value at time "infinity," i.e. the fundamental value, do not equal the market price. These are the only two price bubbles possible in discrete time models. The discrete time bubbles literature mentioned earlier focuses on type 2 bubbles. Lastly, a type 3 bubble exists only in continuous trading models and it corresponds to an asset whose price process is a local martingale but not a martingale. In economic terms, the risk-adjusted expected discounted cash flows and liquidation value at any future finite time, i.e. the fundamental value, does not equal the market price. We study type 3 bubbles. Importantly, type 2 and 3 bubbles capture distinct economic phenomena.

Type 2 bubbles studied within infinite horizon models compare the market price of an asset to its fundamental value, estimated using a model for the asset's dividends and discount rate. This approach encounters three difficulties. One, because the model has an infinite horizon, the model estimation requires a large sample, and that creates a trade-off between the model asymptotics and possible structural breaks in the market.[13] Two, because there is no consensus on how to model and estimate the fundamental value, the traditional approach faces a joint-hypothesis problem. Three, the existing literature on bubble detection mainly exploits information contained in historical prices. However, this backward-looking methodology implicitly assumes time series stationarity. Given the forward-looking nature of bubbles (buy to resell), the stationarity assumption may not be satisfied (unless strong and perhaps unrealistic assumptions are imposed).

In contrast, a type 3 bubbles capture short-term trading strategies designed to capture an

[13]Type 2 bubbles reflect the abstract notion of a liquidation value at time equal to infinity, and the fundamental value is its expected value today. Such an abstract notion of a liquidation value is problematic/debatable.

asset's resale value at a future date. This implies that type 3 bubbles can be estimated using data over short time periods. In particular, our approach allows us to detect the presence of a bubble and quantify its magnitude, simply by observing the prices of options on any given day, without resorting to historical or backward-looking time windows. Finally, notice that, although our estimation procedure is still potentially affected by a joint-hypothesis problem, in contrast to the traditional approach our three-step procedure allows for an independent validation of the fundamental value before testing for bubbles. The accuracy of an option's fundamental value is assessed in the first step of our three-step approach.

Similar to our paper, Jarrow and Kwok (2020) also attempts to detect price bubbles using options data. Although both papers use insights from Jarrow et al. (2010) to identify price bubbles, the approaches are quite different. Jarrow and Kwok (2020) assume that the market satisfies no free lunch with vanishing risk (NFLVR) but not no dominance (ND)[14] and they estimate the asset's price bubble using a non-parametric approach. Their method introduces a truncation bias into their bubble estimates due to the limited range of call and put strikes, which they provide an adjustment for. In contrast, we assume both NFLVR and ND within a flexible parametric model for the underlying asset price evolution. While the joint assumption of NFLVR and ND assures that European put-call parity holds on observed market prices, the parametric model has three advantages: (i) it enables an independent validation of an option's fundamental value (as explained in Section 3.2), (ii) it avoids the truncation bias in their procedure, and (iii) it allows us, using stock price data, to validate our estimated option price bubbles by seeing if the underlying process's parameters are consistent with the existence of stock price bubbles (see Section 5.4). The two papers provide consistent evidence on the existence of stock price bubbles.

We also contribute to the empirical option-pricing literature, which usually employs models with stochastic volatility and jumps, as in Andersen et al. (2015), which belong to the affine family, as described in Duffie et al. (2000). However, by construction, these models do not allow for the existence of option bubbles. Here, we introduce the G-SVJD model, which subsumes many of the models used in the option-pricing literature as special cases. In particular, the G-SVJD is a superset of the affine family and it also allows for non-affine dynamics. The estimation results of the G-SVJD on option data reveal strong evidence against the affine model specification.

This paper also adds to the literature using option prices to infer characteristics of the underlying asset process. For example, Carr and Wu (2003) use time decay in option prices

[14]Both assumptions are discussed in Section 2.

to detect continuous and discontinuous components, Medvedev and Scaillet (2007) relate the slope of the implied volatility of short-term at-the-money options to estimate the leverage effect. More recently, Todorov (2019) uses a cross-section of options with short maturities to nonparametrically estimate the asset's volatility, while Bandi et al. (2021) use short-term options to estimate an asset's volatility, leverage effect, and volatility of volatility. Here, we use put-call parity and the existence of bubbles in call options, as distinct from put options, to determine whether the underlying price exhibits a bubble.

The rest of the paper is organized as follows. Section 2 presents the theory of call option bubbles, while Section 3 describes our estimation procedure. Section 4 describes the data and Section 5 presents the results of the empirical analysis. In Section 6 we apply our estimation approach to GameStop. Section 7 concludes.

2 A Theory of Call Option Bubbles

In this section we review the local martingale theory of bubbles and present the analysis of call option bubbles that underlies our empirical methodology. The local martingale theory of bubbles was developed in a sequence of papers by Loewenstein and Willard (2000b), Loewenstein and Willard (2000a), Cox and Hobson (2005), Heston et al. (2007), and Jarrow et al. (2010). This theory extends the characterization of bubbles from discrete time, infinite horizon models to continuous time, finite and infinite horizon models. It is shown that rational bubbles can exist in an arbitrage-free and frictionless market (see Jarrow (2015) for a review of this literature). This approach enables the use of continuous time stochastic process theory to estimate and test for the existence of asset price bubbles, which is the purpose of our paper.

2.1 The Market

We consider a continuous time, continuous trading model on a finite horizon $[0, T]$ given a complete filtered probability space $(\Omega, \mathcal{F}, \mathbb{F}, \mathbb{P})$. Continuous time is selected because continuous time allows for more types of asset price bubbles to exist within the model, and discrete time can be considered as a special case.[15] The markets are assumed to be frictionless, competitive, and initially with trading in two assets: a risky asset (stock) and a money market account (mma) that is locally riskless. By frictionless we mean that there are no transaction

[15] A discrete time model can be obtained by setting the price process to be a constant between successive time points.

costs nor trading constraints (e.g. short-sale restrictions). By competitive we mean that traders act as price takers.

The market price of the risky asset is given by a non-negative semimartingale $\mathbb{S}_t$.[16] We denote the time t value of mma as $B_t = e^{\int_0^t r_s d_s}$ where r_t is the default-free spot rate of interest. Finally, without loss of generality, in the remainder of the paper we consider the normalized (discounted) asset price $S_t = \frac{\mathbb{S}_t}{B_t}$, i.e. the asset price denominated in units of the numeraire (mma). For simplicity, we assume that no dividends are paid on the underlying stock (we relax this assumption in Section 3).

We assume that the economy satisfies no free lunch with vanishing risk (NFLVR). This is a technical extension of the standard no-arbitrage assumption. Under NFLVR, by the first fundamental theorem of asset pricing, there exists a probability measure $\mathbb{Q}$, equivalent to $\mathbb{P}$, under which the risky asset price process is a local martingale. A local martingale is a stochastic process such that, when stopped on a sequence of stopping times approaching infinity, the stopped process is a martingale.[17] $\mathbb{Q}$ is called an equivalent local martingale measure (ELMM). We do not assume that the market is complete. In an incomplete market, there are infinitely many such ELMMs. To uniquely value options, we assume that the market chooses a unique ELMM.[18] For example, with sufficient options trading, the extended market is complete, which results in a unique ELMM. An alternative is to invoke a representative trader's equilibrium which uniquely determines an ELMM (see Jarrow (2015)).

Given the unique ELMM $\mathbb{Q}$ chosen by the market, the fundamental value (FV) of the asset at time t is defined as

$$FV_t = S_t^* = E_t[S_T], \tag{1}$$

where $E_t[.] = E^{\mathbb{Q}}[.|\mathcal{F}_t]$. This is the expected (risk-adjusted) discounted cash flow from liquidating the stock at the model's horizon, time T. Alternatively stated, it is the value agents would pay if, after purchase, they had to hold the stock until liquidation. This fundamental value is consistent with the standard definition of fundamental value used in the classic economics literature (see Jarrow (2015), Jarrow (2021)). Indeed, a representative trader's ELMM, in an economic equilibrium, is consistent with this definition.[19]

[16] For simplicity of presentation, we omit the necessary measurability and integrability conditions on the assumed price processes; see Jarrow (2021) for these details.

[17] For the formal definition of a local martingale see Jarrow (2021).

[18] A sufficient condition for this selection is that the market is in equilibrium or that the market studied is embedded in a larger market, which includes options, where this embedding uniquely determines the ELMM (see Jacod and Protter (2010)).

[19] An alternative definition of an asset's fundamental value appears in the literature (see Heston et al. (2007), Herdegen and Schweizer (2016), Loewenstein and Willard (2013)), which is the super-replication cost of creating the asset's payoffs. In a complete market the two definitions agree, however, in an incom-

In what follows, quantities with a "*" superscript will denote fundamental values, while those without will denote market prices. Given the above, the asset's price bubble is:

$$\beta_t = S_t - S_t^*. \tag{2}$$

This is the classic notion of a bubble, a deviation of the market price from its fundamental value. Further, for any $t \leq t + \tau \leq T$, we have that

$$S_t = E_t[S_{t+\tau}] + (\beta_t - E_t[\beta_{t+\tau}]). \tag{3}$$

It follows directly that an asset price bubble exists (i.e. $\beta_t > 0$) if and only if the discounted stock price process S_t is a strict local martingale – a local martingale which is not a martingale. This implies that the bubble component β_t is also a strict local martingale. Since a local martingale bounded below is a supermartingale, β_t is also a non-negative supermartingale, declining in expectation over time with $\beta_T = 0$ at the terminal time T. In fact, if a bubbles exist, $(\beta_t - E_t[\beta_{t+\tau}]) > 0$ for any $t \leq t + \tau < T$ in equation (3). Figure 2 provides a graphical depiction of Equation (3).

The figure shows that using options with time-to-maturity $\tau < T$ one can detect the existence of a bubble, and that the magnitude of the estimated bubble is positively related to the option's maturity. Hypothetically, if one could observe options with maturity $\tau = T$, then the option market could, in principle, reveal the full extent of the bubble in the underlying asset, however this is impossible in practice.[20] This implies that for a given τ our estimates can be interpreted as a lower bound on the size of the bubble. The tightness of the bound will depend, among other things, on the difference $T - \tau$. Lastly, as formally shown in Section 2.2.2, while the bubble depends on the option's time-to-maturity it is independent of the option's strike price. This implies that the largest *call option bubble* that one can detect is bounded above by the lowest option price observed across a given set of strikes. This apparently tight upper bound, however, needs to be understood with respect to two distinct aspects: first, for large strikes, the market for call options is generally very illiquid with large bid/ask spreads. Quotes for such deep out of the money options are generally not deep and might not be fully representative of the underlying market. Second, and more

plete market the super-replication cost corresponds to choosing the ELMM that yields the largest value in expression (1) (see Jarrow (2021)). Our market selected ELMM, therefore, is less than or equal to the super-replication cost implying a potentially larger bubble using our definition. This would be the case, for example, using the ELMM determined in a representative trader equilibrium.

[20] Recall that T corresponds to the horizon of the model which is not know.

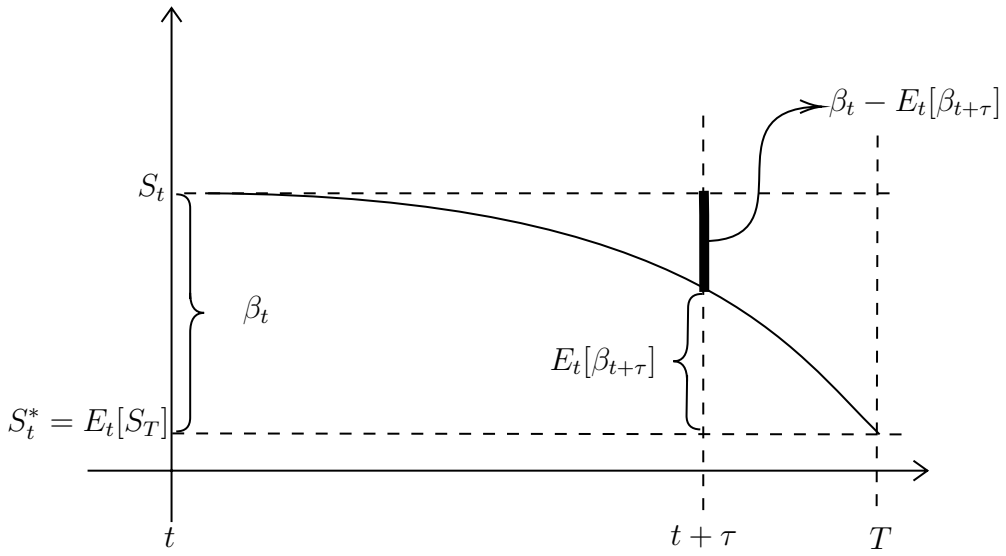

Figure 2: Graphical Representation of Equation (3)

importantly, as formally shown in Appendix C, even small bubbles detected over a short horizon (i.e. using short maturity options), can be the reflection of a much larger bubble over longer horizons.

Necessary and sufficient conditions on the asset's stochastic process' local characteristics to be a strict local martingale are known only for a handful of stochastic processes (see Jarrow et al. (2020) for a collection of such processes). For example, if the price process is represented by $dS_t = \sigma(S_t)dW_t$ where W_t is a standard Brownian motion and $\sigma(S)$ is the stock's volatility, then S_t is a strict local martingale under the ELMM $\mathbb{Q}$ if and only if $\int_\epsilon^\infty \frac{s}{\sigma^2(s)}ds < \infty$ for some $\epsilon > 0$ (see Delbaen and Shirakawa (2002), also see Jarrow (2021), chapter 3). This example implies that a bubble exists if and only if the local volatility increases faster than the stock price level S_t, so that above integral is finite. This intuition, that bubbles are generated by increasing volatility as the stock price increases, is quite general[21] and utilized below to help explain our empirical results.

2.2 Call Option Bubbles

We now present the theory of option valuation in a market with price bubbles. We augment the market to include trading in call and put options with various strikes and maturities, and default-free zero-coupon bonds of various maturities. Let $K = \frac{\mathbb{K}}{B_{t+\tau}}$ denote the strike

[21] In fact, it can be shown that a price bubble exists when an asset's quadratic variation (volatility) explodes (equals infinity) with positive probability over the model's horizon, implying the underlying price process hits zero.

price in units of the mma on an option (call or put) with expiration date $t+\tau$. Let $C_t(K,\tau)$ and $P_t(K,\tau)$ denote the market prices, in units of the mma, of the call and put options, respectively, observed at time t with strike price K and maturity τ. At expiration, the call and put option payoffs are equal to $C_{t+\tau}(K,0) = max\{S_{t+\tau} - K, 0\}$, and $P_{t+\tau}(K,0) = max\{K - S_{t+\tau}, 0\}$, respectively. In what follows, in order to simplify the notation, we often remove the option dependency from strike price and maturity. However, this should cause no confusion in that the strikes and maturities will be obvious in such cases. Finally, let $p(t,\tau)$ denote the time t dollar value of a default-free zero-coupon bond paying a dollar at time $t+\tau$.

We assume that the augmented market, including trading in the options and zero-coupon bonds, satisfies NFLVR, i.e. is arbitrage-free. As before, invoking the first fundamental theorem of asset pricing, this implies that the option market prices, $C_t(K,\tau)$ and $P_t(K,\tau)$, and the normalized zero-coupon bond prices $\frac{p(t,\tau)}{B_t}$ are all $\mathbb{Q}$ local martingales. The next questions investigated are the existence and characterization of price bubbles in these additional traded securities. Although these results are known, we repeat them here to make the exposition self-contained.

2.2.1 Zero-coupon Bonds

Analogous to the risky asset's fundamental value, we define the fundamental value of a zero-coupon bond, in dollars, as

$$p^*(t,\tau) = E_t\left[\frac{1}{B_{t+\tau}}\right] B_t.$$

This corresponds to the discounted (and risk adjusted) dollar payoff at time $t+\tau$.

To simplify the analysis, we assume that interest rates are non-negative, i.e. $p(t,\tau) \leq 1$ for all $0 \leq t \leq t+\tau \leq T$. Given this assumption, the following theorem shows that zero-coupon bond prices have no bubbles. This follows directly from the fact that local martingales uniformly bounded above are martingales.

Theorem 1 (No Zero-coupon Bond Price Bubbles)**.** *Assume* $p(t,t+\tau) \leq 1$ *for all* $0 \leq t \leq t+\tau \leq T$. *Then,* $p(t,\tau) = p^*(t,\tau)$.

The proof is contained in Appendix B. Intuitively, a bubble in any asset can exist only when the asset can be bought with the expectation that it can be sold in the future at a higher price. But, if the price of the asset (or option) is bounded above, then at some future time this can no longer happen. By backward induction, rational traders will realize this

possibility at earlier times as well, and the motive for this purchase disappears at all earlier times.

2.2.2 European Options

First, we consider European options. As before, the fundamental values of European put and call options (all in units of mma) are defined by the following expressions:

$$P_t^{E^*} = E_t\left[P_{t+\tau}\right] \quad \text{and} \quad C_t^{E^*} = E_t\left[C_{t+\tau}\right], \tag{4}$$

which correspond to the expected (after risk adjustment) discounted payoffs of the options at maturity. We discuss the following three theorems whose proofs are contained in Appendix B.

Theorem 2 (European Puts Have No Bubbles)**.** *Assume* $p(t,\tau) \leq 1$ *for all* $0 \leq t \leq t+\tau \leq T$. *Then,* $P_t^E = P_t^{E*}$

The intuition behind Theorem 2 is analogous to that behind Theorem 1 – because a put's payoff is bounded above, puts do not have bubbles. However, because a European call option's payoffs are unbounded above, the same argument does not apply to call options. We have the following theorem:

Theorem 3 (European Calls Can Have Bubbles)**.** $C_t^E = C_t^{E*} + \delta_t(\tau)$ *where* $\delta_t(\tau) \geq 0$ *is a supermartingale with* $\delta_{t+\tau}(\tau) = 0$. *If* $\delta_t(\tau) > 0$, *then there is a bubble.*

As shown, European call options can have bubbles, independent of the underlying risky asset price process, and the call option's bubble must disappear at the option's maturity.

To relate the call option's bubble to the bubble in the underlying asset, we add another assumption. We assume that the economy satisfies no dominance (ND) – originally used by Merton (1973). ND is a stronger assumption than NFLVR but much weaker than assuming market equilibrium. ND means that there is no trading strategy that can be constructed whose future payoffs and cost of construction dominate any single asset's future payoffs and current price.[22] In an economy that satisfies only NFLVR, ND can be violated. The key implication of this assumption for the subsequent theorem is that ND implies put-call parity holds,[23] i.e.

$$C_t^E - P_t^E = S_t - Kp(t, t+\tau). \tag{5}$$

[22] For a more technical discussion see Jarrow et al. (2010) and Jarrow (2021).

[23] A generalized version of put-call parity, involving inequalities, holds for American options as well.

Note K is in units of the mma, so only $p(t, t+\tau)$ appears here. It is well known that European put-call parity is rarely violated empirically, so this additional assumption is not that restrictive.[24] This assumption implies the following theorem:

Theorem 4 (Call Bubbles and Asset Price Bubbles)**.** *Assume ND, then*

$$C_t^E = C_t^{E^*} + \beta_t - E_t\left[\beta_{t+\tau}\right]. \tag{6}$$

Or, equivalently $\delta_t(\tau) = \beta_t - E_t\left[\beta_{t+\tau}\right]$*, which is independent of* K*.*

Note that under NFLVR and ND, the call option's bubble is linearly related to the underlying asset's price bubble, and it is independent of the option's strike price. This means that different strike options with the same maturity should exhibit the same bubble. The magnitude of the call option's bubble vanishes in the limit as the option's maturity τ reaches zero since $E_{t+\tau}[\beta_{t+\tau}] = \beta_{t+\tau}$. Finally, we see that call option's bubble provides a lower bound $\beta_t - E_t[\beta_{t+\tau}]$ on the asset's price bubble. We use this fact below when designing a test for detecting asset price bubbles using call options with maturity τ.

Finally, it is important to state that under both NFLVR and ND, this theorem gives a necessary and sufficient condition for the existence of a call option bubble, which is that the underlying asset price must have a bubble, i.e. $\beta_t > 0$. This is true if and only if the underlying process is a supermartingale. If ND is violated, then the linear relation in expression (6) need not hold and the call option's and stock price's bubbles are unrelated. For example, the stock price may not exhibit a bubble, but the call option can, and conversely.

2.2.3 American Options

Payoffs for American puts are bounded above, so their valuation follows the well-known results from standard option-pricing theory formulated without the inclusion of price bubbles. But again this is not true for American calls. Given no dividends on the underlying asset, we have the standard result (which simply follows using ND) that

$$C_t^A = C_t^E, \tag{7}$$

because an American call option is never exercised early. In conjunction, the two previous equations imply that an American call option's bubble is also linearly related to the asset's bubble,

[24] We note that for large strike options which trade with less liquidity, put-call parity is less likely to be satisfied, suggesting that this relation is more likely to hold for strike prices near the money.

$$C_t^A = C_t^{E^*} + \beta_t - E_t\left[\beta_{t+\tau}\right]. \tag{8}$$

This means that even in the case of an American call option we can use the price of the corresponding European-style option to *identify* and *quantify* the presence of a stock-price bubble.[25]

2.3 Bubble Estimation

Sections 2.2.2 and 2.2.3 show how call option bubbles can be used to identify bubbles in the underlying asset's price. Specifically, Equations (6) and (8) show that a lower bound on the asset's price bubble is given by the call option's bubble (either European or American, which we denote by $C_t^{E/A}$).

The above relations allow us to define a simple procedure for identifying the existence of a call option price bubble that entails three steps. (I) First, we specify a parametric model for the underlying asset S_t under the risk-neutral measure $\mathbb{Q}$. This amounts to specifying a parameter vector θ that governs the dynamics of the asset which, in conjunction with the observed underlying price S_t, allows us to generate model-implied put option prices, $P_t^E(\theta)$; (II) second, we estimate the parameter vector θ by minimizing the distance between observed, either European or American, put prices ($P_t^{E/A}$), and option-implied European Put option prices ($P_t^E(\theta)$). It is crucial for this step that observed put market prices do not exhibit bubbles, as discussed in Section 2.2; (III) third, we use the parameter vector estimated in the previous step, $\hat{\theta}$, to compute model-implied European call option prices ($C_t^{E^*}(\hat{\theta})$) that are generated under the risk neutral measure and which represent the calls' fundamental value, that is $C_t^{A^*/E^*} \approx C_t^{E^*}(\hat{\theta}, K, \tau)$.

We estimate the call option price bubble as the difference between the observed call market price ($C_t^{A/E}(K,\tau)$) and its fundamental value (which is given by the call model price $C_t^{E^*}(\hat{\theta}, K, \tau)$):

$$\mathcal{B}_t(K,\tau) = \beta_t - E_t[\beta_{t+\tau}] = \left(C_t^{A/E}(K,\tau) - C_t^{E^*}(\hat{\theta}, K, \tau)\right) \times 100. \tag{9}$$

[25] Equation (8) is derived under the assumption that in addition to American calls trading, both European calls and puts trade. If only American calls and puts trade, then the above expression is only approximately true, the difference bounded by $\max\{(P_t^A - P_t^E), \left|(P_t^A - P_t^E) - K(1 - p(t,t+\tau)\right|\}$. Put-call parity for European options is $C_t^E - S_t = P_t^E - Kp(t,t+\tau)$. Put-call parity for American options is $P_t^A - K \leq C_t^A - S_t \leq P_t^A - Kp(t,t+\tau)$. But, because $C_t^A = C_t^E$, we have

$$P_t^E + (P_t^A - P_t^E) - Kp(t,t+\tau) - K(1 - p(t,t+\tau)) \leq C_t^E - S_t \leq P_t^E + (P_t^A - P_t^E) - Kp(t,t+\tau).$$

The errors on the left and right sides are at most: $(P_t^A - P_t^E) - K(1 - p(t,t+\tau))$ and $(P_t^A - P_t^E)$, respectively.

Notice that we multiply the bubble magnitude by 100, because one standardized option contract is equivalent to owning 100 shares of the underlying stock.[26] As seen above, a price bubble exists in the underlying asset if and only if there exists a call price bubble (under the joint assumptions of NFLVR and ND).

Even if in step (I) the asset's price parameters are sometimes measured with large standard errors (because some of them have similar effects on the underlying asset's distribution), the option's fundamental values in step (II) are estimated with great precision. This difference in precision is analogous to using a linear regression with a large R^2, where the independent variables are highly correlated (a multicollinearity problem). This is the reason we utilize option price data, and not stock price data, to test for the existence of stock price bubbles. We will return to this issue below.

It should be noted that our identification strategy crucially depends on the parametric model specified in step (I). As such, the above testing procedure for identifying the presence of a bubble would seem to be affected by the so-called joint-hypothesis problem. Fortunately, step (II) of our procedure allows us to mitigate the potential concerns about model misspecification as the quality of the pricing fit on put options provides a direct validation of the model. This enables us to decouple the testing of the specific option-pricing model from the subsequent tests for the existence of a bubble in the underlying asset. In Section 3 we describe in detail how the above procedure can be implemented using either European or American options.

3 The Estimation Procedure

We now discuss the implementation of the three-step estimation procedure described in Section 2.3.

3.1 Step I: The Model

This section presents the parametric model used for our empirical analysis. The crucial requirement is that the parametrized process for the underlying asset needs to admit both martingale and strict local martingale possibilities. This requirement rules out many well-known processes such as those with independent increments (e.g. Levy processes), the Mer-

[26] Also, to obtain the magnitude of the option price bubble in dollars, we should multiply Equation (9) by the value of the mma, B_t. However, by setting the current time t as the initial time, where $B_t = 1$, this adjustment is not needed.

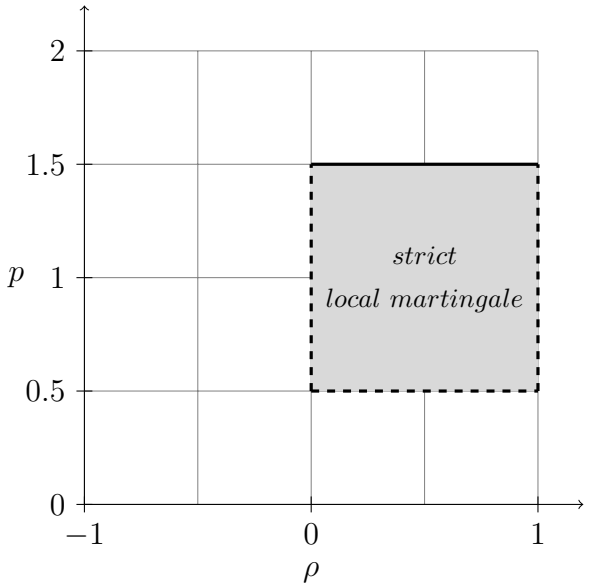

Figure 3: **G-SVJD model**: The gray area represents the parameter space that makes the model in equation (12) and (13) a strict local martingale.

ton (1976) jump diffusion, the Heston (1993) stochastic volatility, the Bates (1996) model, and affine jump-diffusion models (see Duffie et al. (2000)).

There are a limited number of known candidate processes (see Jarrow et al. (2020)). We select the following stochastic volatility model under the ELMM $\mathbb{Q}$:[27]

$$dS_t = S_t\sqrt{V_t}dW_t \tag{10}$$

$$dV_t = \kappa(\bar{\nu} - V_t)dt + \sigma_v V_t^p dZ_t \tag{11}$$

where W_t and Z_t are correlated standard Brownian motions with $\rho \in [-1, 1]$ such that $dW_t dZ_t = \rho dt$, $\sigma_v > 0$ is the volatility of the variance process V_t (i.e. vol of vol), $\kappa > 0$ is the mean-reversion speed of the variance process, and $\bar{\nu} > 0$ is the long-term mean of the variance.

Figure 3 shows the varying combinations of the parameters p (which enters Equation (11) by affecting the volatility of volatility) and the correlation coefficient between the Brownian increments, ρ, that jointly govern whether the stock price is a strict local martingale or just a martingale under $\mathbb{Q}$. Specifically, from the results in Andersen and Piterbarg (2007) and Lions and Musiela (2007), we know that:

(i) when $p \leq 1/2$ or $p > 3/2$, S_t is a martingale;

[27]Since the normalized stock price is $S_t = \frac{\mathbb{S}_t}{B_t}$, applying integration by parts, we get $\frac{dS_t}{S_t} = \frac{d\mathbb{S}_t}{\mathbb{S}_t} - r_t dt$. Hence, we obtain the discounted price evolution by removing the riskless drift term rdt.

(ii) when $1/2 < p < 3/2$, S_t is a martingale for $\rho \leq 0$ and a strict supermartingale (and hence a strict local martingale) for $\rho > 0$.[28]

As discussed above, the intuition for the existence of an asset price bubble is that the stock's volatility increases at a faster rate than its price, resulting in explosive behavior in the stock's volatility process. In our case, this intuition holds true under the parameter restrictions (i)-(ii). This "non-linear" combination of parameter values for the existence of a bubble results from a tradeoff induced by the parameters ρ and p. Under condition (i) for parameter p, the volatility is not explosive enough relative to the stock price even if $\rho > 0$. In contrast, under condition (ii), $\rho > 0$ results in explosive behavior in the stock's volatility relative to the stock price increase.

While the processes in Equations (10) and (11) are technically sufficient for our purposes, a large body of asset-pricing literature highlights the importance of price jumps, especially when confronting a model with option prices and the corresponding high level of implied volatilities for out-of-the-money options (see Merton (1976), Bates (1996), and more recently Andersen et al. (2015)). To address concerns about model misspecification, we augment the model by adding an independent and discontinuous martingale to Equation (10) above. Adding a martingale to a strict local martingale retains the strict local martingale behavior of the original process, so the parameter values of the original diffusion process will still govern the existence, or lack thereof, of bubbles. Thus, we consider the following generalized stochastic volatility jump-diffusion (G-SVJD) model:

$$\frac{dS_t}{S_t} = \sqrt{V_t} dW_t + dJ_t - \lambda M dt \tag{12}$$

$$dV_t = \kappa(\bar{\nu} - V_t)dt + \sigma_v V_t^p dZ_t \tag{13}$$

where $(dJ_t - \lambda M dt)$ is the martingale jump term, $dJ_t = d\left(\sum_{j=1}^{N_t}(Y_j - 1)\right) = (Y_t - 1)dN_t$ with Y_i being i.i.d random variables representing the price jump size, with $Y_j \sim \mathcal{LN}(\mu_y, \sigma_y)$ such that $log(Y_j) \sim \mathcal{N}(\mu_y, \sigma_y)$. $N_t \sim Poisson(\lambda t)$ is the counting process with intensity given by λ counting the total number of jumps up to time t. Finally, $J_t - \lambda M t$ is a martingale with $M = E[Y_j - 1] = e^{(\mu_y + 0.5\sigma_y^2)} - 1$ being the jump's compensator. Note that jumps in volatility cannot be added to the G-SVJD model. Volatility jumps would affect the

[28] Further, when $p = 3/2$, S_t is a martingale for $\rho \leq \frac{1}{2}\sigma_v$ and a strict supermartingale for $\rho > \frac{1}{2}\sigma_v$ (see Andersen and Piterbarg (2007) for more details). Because this condition involves an exact value of the parameter p, in what follows we focus on conditions (i) and (ii), which involve parameter ranges and thus are empirically more relevant.

current stock price evolution and invalidate this model of bubble identification. As discussed above, only a handful of stochastic (volatility) processes are currently known with a complete characterization of their martingale/strict local martingale behavior. The G-SVJD model is arguably quite general within this class of processes, and it is also the closest to processes employed successfully in previous option-pricing empirical studies.[29]

3.2 Step II: Model Estimation

Given the above G-SVJD model, we now discuss the parameter estimation. Because closed-form or analytical expressions for the price of European options (i.e. the call's fundamental values) are not available, we resort to Monte Carlo simulation. Specifically, we simulate MC trajectories from the discretized versions of the model in Equations (12) and (13) according to:

$$V_{i,t+\Delta t} = V_{i,t} + \kappa(\bar{\nu} - V_{i,t})\Delta t + \sigma_v V_{i,t}^p \sqrt{\Delta t} B_{i,1} \tag{14}$$

$$S_{i,t+\Delta t} = S_{i,t} \exp\left[-\left(\lambda M + \frac{1}{2}V_{i,t}\right)\Delta t + \sqrt{V_{i,t}\Delta t}\left(\rho B_{i,1} + \sqrt{1-\rho^2} B_{i,2}\right) + \mathcal{J}\right], \tag{15}$$

where $B_{i,1}$ and $B_{i,2}$ are independent standard normal variables, for $i = 1, \cdots, MC$ and $\Delta t = \frac{1}{365\times 5}$.[30] The model-implied put price $P_t(\theta, K, \tau)$ for strike K and maturity τ is obtained from the simulated prices $\{S_{i,t+\tau}\}_{i=1,\cdots,MC}$ as:

$$P_t(\theta, K, \tau) = \frac{1}{MC}\sum_{i=1}^{MC}(K - S_{i,t+\tau})^+. \tag{16}$$

If the underling asset pays a dividend yield we transform the price process S_t by augmenting it by the dividend yield earned over the maturity of the option, i.e. $\tilde{S}_t = S_t e^{\delta t}$. The new stock price $\tilde{S}_t$ will be S_t plus accumulated dividends, i.e.

$$\frac{d\tilde{S}_t}{\tilde{S}_t} = \frac{dS_t}{S_t} + \delta dt \tag{17}$$

Equation (17) transforms the asset with cash flows into an equivalent asset without cash flows by reinvesting all cash flows into the risky asset itself (see Jarrow (2021)). Price trajectories

[29] In particular, note that the G-SVJD nests several well-known models as special cases: (i) the Merton (1976) model for $\sigma_v = 0$, (ii) the Heston (1993) model for $p = 0.5$ and $\lambda = 0$, and (iii) the Bates (1996) model for $p = 0.5$ and $\lambda > 0$.

[30] This amounts to simulating the process in five time steps each day, or every 4.8 hours.

for $\tilde{S}_t$ can be generated following the same discretization scheme outlines in Equations (14) and (15). Finally, European put option prices are computed following a standard risk neutral valuation as follows:

$$P_t(\theta, K, \tau) = \frac{1}{MC} \sum_{i=1}^{MC} (K - \tilde{S}_{i,t+\tau} e^{-\delta(t+\tau-t)})^+.$$

where $\tilde{S}_{t+\tau} e^{-\delta(t+\tau-t)}$ represents the value without accumulated dividends over $(t, t+\tau)$, because the option holder does not receive the dividends paid over the option's life.[31]

The G-SVJD model has a total of 9 parameters, many of which have similar affects on the underlying's distribution:

$$\theta = \{V_0, \bar{\nu}, \kappa, \sigma_v, \rho, p, \mu_y, \sigma_y, \lambda\}.$$

As in Andersen et al. (2017) we estimate the parameter vector on each day t using one option's maturity per-date.[32] As explained in Section 4, on each day we select the maturity date (between 7 and 50 calendar days) with the highest cumulative traded volume in put options.[33] This step is done to ensure that put-call parity is more likely to hold in the observed market prices. Hence, for each underlying asset we obtain a sequence of parameter vectors $\{\theta_t\}_{t=1,\cdots,T}$, where T represents the total number of days in our sample. We estimate θ_t as in Andersen et al. (2017)[34] by minimizing the root mean squared errors between market and model Black-Scholes implied volatilities ($RMSE_{IV}$), i.e.:

$$\hat{\theta} = \min_{\theta_t} \sqrt{\frac{1}{N_t^p} \sum_{n=1}^{N_t^p} \left[IV_t(K_{t,n}, \tau_t) - IV_t(\theta_t, K_{t,n}, \tau_t) \right]^2} \tag{18}$$

where N^p is the number of market put prices on date t with strike price $K_{t,n}$ and maturity τ_t.

[31] For dividend-paying individual stocks, our approach applies unchanged to American put options. For American call options on stocks that pay dividends, our approach can be extended in piecewise fashion to options whose maturity dates are prior to the next ex-dividend date.

[32] Ideally, at the estimation stage, one could use a few day window over which the parameters are kept constant, allowing only the spot volatility to change day-by-day. Also, one could price options with multiple maturities on a given day. While these alternatives are worth exploring, the computational complexity that they entail would make the estimation infeasible given that option values can only be computed via simulation. Choosing the most liquid cross-section on any given day, and re-estimating the parameters every day, strikes a balance between robustness and computational feasibility.

[33] Call options also experience similarly high volumes on these very dates.

[34] The estimator in Equation (18) and its corresponding asymptotic theory relies on the assumptions of a fixed time span and an increasing number of options within a cross section. Details can be found in Andersen et al. (2015) and Andersen et al. (2019).

Note that N^p comprises both ITM and OTM put options which span the entire support of the risk neutral distribution. Finally, $IV_t(K_{t,n}, \tau_n)$ and $IV_t(\theta_t, K_{t,n}, \tau_t)$ are the implied volatilities of the market and model-implied put prices $P_t(K_{t,n}, \tau_t)$ and $P_t(\theta_t, K_{t,n}, \tau_t)$, respectively. We minimize implied volatilities instead of prices because doing so normalizes the objective function across strikes/maturities and the errors are interpretable as volatility percentages (see Christoffersen and Jacobs (2004) for more details on the choice of this type of an objective function).[35]

We emphasize again that this sum of squared minimization gives very accurate option values, even though the parameter estimates for some assets have large standard errors, due to the similar impacts that many of the parameters in θ have on the underlying asset's price distribution. Nonetheless, to reduce the dimension of the parameter space and help parameter identification (since we only use only one option maturity per day in our estimation) we apply the following parameter restrictions to discipline the identification of $V_{0,t}$, κ_t, and $\bar{\nu}_t$. First, we fix the speed of mean reversion at $\kappa_t = 5$, which corresponds to 22 days half-life of the variance process, which is comparable to what has been estimated in the option-pricing literature.[36] Second, we set $\bar{\nu}_t = IVATM_t^2$, where $IVATM_t$ is the implied volatility of the option closest to at-the-money on day t.

As explained in Section 2, the identification of a bubble in the underlying asset hinges on the value of the parameters ρ and p. To understand how call option prices and their corresponding implied volatilities help in identifying these parameters, Figure 4 shows the implied volatility generated by our model as a function of strike prices for varying values of ρ and p. From the left Panel of Figure 4 we can see that the correlation coefficient ρ is identified by the slope of the implied volatility of the options that are around at-the-money. A negative (positive) ρ is associated with a downward (upward) sloping IV curve (around at-the-money). From the right Panel of Figure 4 we see that the parameter p, which affects the volatility of volatility of the price process, affects the thickness of the tail of the return's risk-neutral distribution (i.e. its kurtosis), which is then reflected in the concavity of the IV curve.

[35] We impose the Feller condition $\sigma_{v,t}^2 \leq 2\kappa_t\bar{\nu}_t$ to ensure the non-negativity of the variance process V_t.

[36] In unreported results, available upon request, we confirm that the size of the estimated bubble is only marginally affected by the speed of mean reversion of the variance process.

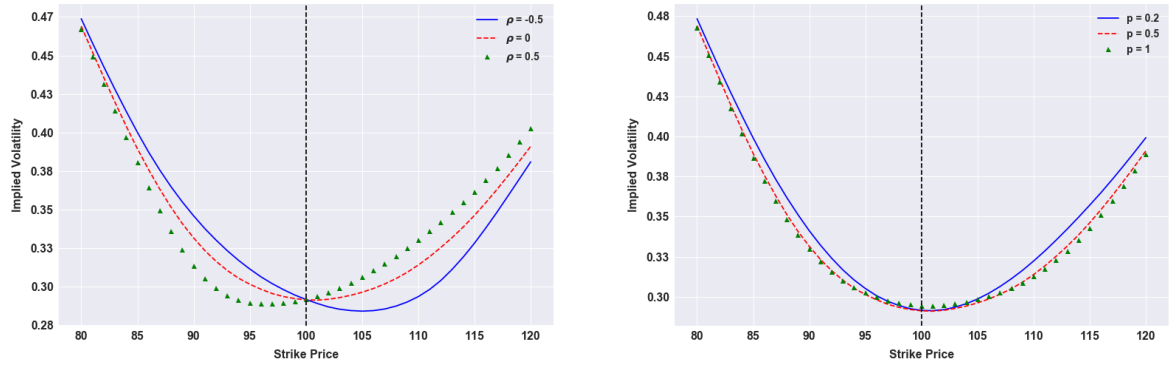

Figure 4: **Parameter Identification**: The left (right) Panel shows the implied volatility generated by the G-SVJD model in equations (13) and (12) for varying values of the parameters ρ and p. We set the remaining parameters to their estimated time-series averages for Amazon, as reported in Table 2.

3.3 Step III: Call Option Bubble Estimation

Next, given the estimated parameters $\hat{\theta}_t$, on each day we generate call option prices with maturity τ_t over the set of available strikes $\{K_{t,n}\}_{n=1,\cdots,N_t^c}$ (where N_t^c represents the number of available call options at time t with maturity τ_t). The call option bubble for a given strike $K_{t,n}$ is estimated as:

$$\hat{\mathcal{B}}_t(K_{t,n},\tau_t) = \left[C_t^{A/E}(K_{t,n},\tau_t) - C_t(\hat{\theta}_t, K_{t,n},\tau_t)\right] \times 100. \tag{19}$$

As there are N_t^c call options (which can differ from the number of put options N_t^p), we take the average of the estimated option bubble across the various strikes $K_{t,n}$ within the same maturity τ_t, and we normalize them by the value of the underlying asset. Thus, we define the average call option bubble magnitude as a percentage of the asset value, i.e.

$$\hat{\mathbb{B}}_t = \frac{1}{\mathbb{S}_t}\sum_{n}^{N_t^c}\frac{\hat{\mathcal{B}}_t(K_{t,n},\tau_t)}{N_t^c}. \tag{20}$$

Since options frequently trade within the bid-ask spread but not necessarily at the mid point of the bid-ask spread, it is not clear what the "true" market price is. We take this into account by employing the following classification:

- If the model call price lies between the bid-ask prices, i.e. $C_t^{Bid}(K_{t,n},\tau_t) \leq C_t(\hat{\theta}_t, K_{t,n},\tau t) \leq C_t^{Ask}(K_{t,n},\tau_t)$, we set the call bubble to zero, i.e. $\hat{\mathcal{B}}_t(K_{t,n},\tau_t) = 0$.

- If $C_t^{Bid}(K_{t,n}, \tau_t) > C_t(\hat{\theta}, K_{t,n}, \tau t)$ or $C_t^{Ask}(K_{t,n}, \tau_t) < C_t(\hat{\theta}_t, K_{t,n}, \tau t)$ we compute the call bubble according to Equation (19).

This is a more conservative approach relative to taking differences using market mid-prices and makes our inference more robust to measurement errors and possible liquidity concerns. In the next section we describe how to build formal statistical tests to assess the null hypothesis that the call option's bubble $\mathbb{B}_t$ (or functions of $\mathbb{B}_t$) is equal to zero.[37]

3.4 Testing For Asset Price Bubbles

In this section we formulate a statistical test for the existence of call option bubbles that incorporates both model misspecification and observation error. This test builds on the observation that, in the local martingale theory of bubbles, negative bubbles (i.e. $\mathbb{B}_t < 0$) are precluded because the fundamental value always represents a lower bound on the market price.[38]

Negative bubbles might arise empirically because of two reasons. First, market prices are observed with error. Options, especially OTM options, show significant bid-ask spreads. Moreover, the option and the underlying markets could be affected by asynchronous trading and market participants' trading constraints. Second, we measure the call option's bubble as the difference between the market and the model price. Even though the G-SVJD model underlying the option's value is quite general, possible model misspecification could introduce measurement error. Thus, we interpret negative bubbles as a reflection of the noise caused by the above possibilities.

Given this insight, we develop a statistical test that uses estimated negative bubbles to quantify the distribution of the errors in our option bubble estimates. This distribution is then used to compute confidence intervals to test the null hypothesis of zero call option bubbles. Given the discussion in the introduction, empirically we expect to see bubbles fluctuating in the vicinity of zero most of the times, with occasional large spikes that we can interpret as periods of heightened reselling motives.[39] We build our tests on the following

[37] Our framework assumes frictionless markets, NFLVR, and ND. In reality, there could be instances in which ND and hence, put-call-parity, is temporarily violated. In these cirscumstances, call options could still exhibit bubbles, but they would not represent a lower bound for the asset's price bubble. However, in our methodology the above instances would still indicate non-zero asset price bubble.

[38] Note that some equilibrium models could generate negative bubbles in the presence of trading constraints. However, the economic mechanisms are quite different from those considered here (for example, see Jarrow and Lamichhane (2021)).

[39] More formally, we observe one sample path $\omega \in \Omega$ over a given observation period $t \in [1, T]$, which implies that, given any $t \in [1, T]$, $\mathbb{B}_t(\omega)$ is a constant. Hence, in what follows, we can drop the ω argument.

statistical model:

$$\hat{\mathbb{B}}_t = \mathbb{B}_t + \varepsilon_t,$$

where $\hat{\mathbb{B}}_t$ is the estimate of a call option bubble's magnitude and $\varepsilon_t \sim N(0, \sigma_t)$ represents the model error plus noise. This test is constructed to test the null that the call option bubble is equal to zero on a given day, i.e.

$$(H_0) : \mathbb{B}_t = 0.$$

Of course, under our assumptions, if the call option bubble is zero, the underlying asset's bubble is zero as well. This is the key motivation for using options to test for the existence (not the magnitude) of an asset price bubble. We use σ_t to construct a time-varying threshold. A option bubble is considered significant if it is above this threshold on any given day t. Importantly, since the threshold is estimated using only the available information up to time t, this makes it possible to estimate a call option's bubble in real time.

To implement the above test, σ_t is estimated over a small time window immediately before time t. The estimator relies on the following observation. If $\hat{\mathbb{B}}_t < 0$, then $\mathbb{B}_t + \varepsilon_t < 0$. Since option bubbles must always be non-negative ($\mathbb{B}_t \geq 0$), this implies the error must be negative and large, i.e.

$$\varepsilon_t < -\mathbb{B}_t \leq 0.$$

Under the null, where $\mathbb{B}_t = 0$, the bubble estimate is just the error, i.e. $\hat{\mathbb{B}}_t = \varepsilon_t < 0$. This insight allows us to create an estimator for the variance of the noise process.

Theorem 5 (Bubble Test)**.** *Consider a small time window (equal to k days) before time t. We partition the daily bubble estimates $\{\mathbb{B}_i\}_{i=t-k,\cdots,t}$ into two sets, and only collect observations at times $i = t-k, ..., t$ where $\hat{\mathbb{B}}_i < 0$. Call this set Υ_-. Let the number of elements in this set be N_-. For this set of observations, an unbiased estimator of σ_t^2 is*

$$\hat{\sigma}_t^2 = \sum_{i \in \Upsilon_-} \frac{1}{N_-} \hat{\mathbb{B}}_i^2. \tag{21}$$

Even though under the null hypothesis the observations $\hat{\mathbb{B}}_t > 0$ are also just error, since we observe $\hat{\mathbb{B}}_t > 0$, it must be the case that if bubbles exist, $\mathbb{B}_t > 0$ is larger than any negative errors included within this set (which occur with positive probability, roughly half the time). This implies that including these observations in our σ_t^2 estimator would generate a biased statistic if option bubbles exist, because $\mathbb{B}_t$ itself varies over time.

The above test is meant to be robust towards the effects induced by early exercise premium and market frictions such as stock lending fees. Indeed, when applying our methodology to American put options, we compute prices according to equation (16), which does not account for the early exercise premium. This again is a potential model misspecification. This model misspecification, however, reduces the likelihood of detecting a significant call option bubbles. Indeed, the model misspecification inflates the European puts estimated implied volatility (IV), which in turn inflates the IV of the European call's fundamental value, thereby decreasing the size of the estimated call bubble. A similar argument applies when we consider the possible effect of market frictions such as stock lending fees. Since the presence of stock lending fees increases the cost to short the underlying stock, this has the effect of making it harder to exploit deviation from put-call parity, again leading to potentially inflated put option prices (or implied volatility), which again introduces a negative bias into our bubble estimation.

Finally, is important to emphasize that this statistical test for detecting call option bubbles is independent of the assumption of ND, and is valid even if put-call parity is violated. The assumption of ND is only imposed after all the estimation is completed so that a significant call option bubble implies a significant underlying asset price bubble.

4 The Data

Our empirical analysis focuses on two sets of assets: (i) two broad market indexes, the S&P 500 (ticker: SPX) and Nasdaq-100 (ticker: NDX), and (ii) two individual stocks, Amazon (ticker: AMZN) and Facebook (ticker: FB), which are routinely associated in the financial press with possible price bubbles. Our sample runs from January 2, 2014 through December 31, 2018. The initial date of our sample is dictated by the quality of available option data. As shown in Andersen et al. (2017), over the last decade the equity index option market has exhibited tremendous growth in terms of both trading volume and the number of available contracts. This growth owes, in part, to the introduction of short maturity options, the so-called weeklies. More recently, the popularity of weekly options has expanded from index options to options on individual stocks. Starting our sample in 2014 allows us to have, every day, a sufficient number of options over a wide strike range, which in turn facilitates a robust and reliable implementation of our proposed methodology, as explained in Section 3. This choice of our sample period, the increased market-wide liquidity, makes it more likely that our assumptions NFLVR and ND are consistent with market prices.

We obtain daily end-of-day put and call option quotes from OptionMetrics. On each day, and for each asset, we keep only the cross-section with the highest cumulative volume.[40] The choice of option maturity is dictated by two observations. First, as discussed in Section 2.2.2, because the call option's bubble decreases with the option's tenor, we discard options with very short maturities (i.e. $\tau < 7$). Second, because most of an option's liquidity is concentrated when their maturity shortens, we discard options with maturities longer that 50 calendar days. Again, these filters are included to help ensure consistency of market prices with our assumptions of NFLVR and ND.

Table 1 reports summary statistics for the final option data sample. As can be seen from Table 1, which is relevant to to our empirical analysis, both puts and calls on all four assets span a large and similar standardized moneyness range that covers, at least, the range between -4 and 3. This means that both option types span a large portion of the risk-neutral distribution.

In terms of the number of options, although SPX and NDX on average exhibit a larger number of available contracts with a daily average of around 120 unique strikes, both AMZN and FB also exhibit a large number of quoted options with at least 20 unique strikes per day. Interestingly, for indexes we see more put options than call options, but for single stocks the two option types are equally represented. A similar pattern can be observed in trading interest (i.e. trading volume and open interest). For indexes these are more concentrated in put options while for single stocks these are divided equally between put and call options. The average option maturity is slightly higher for the equity indexes (23 for SPX and 18 for NDX) than for single stocks (15 for AMZN and 17 for FB). This reflects the considerable popularity of standard monthly options for indexes, while weeklies absorb most of the trading volume in equity options. In terms of observation errors, both SPX and NDX have a relative bid-ask spread of around 33% while in AMZN and FB the relative bid-ask spread is around 14%. A possible explanation of the latter fact is that the average at-the-money implied volatility (and, as a consequence, the average at-the-money option price, which enters at the denominator of the relative bid-ask spread) is much lower for indexes (between 12% and 16%) than for single stocks (around 28%). In summary, since our empirical analysis is based on both in- and out-of-the-money put and call options, it is important to note that both option types are available over a large moneyness range with high trading volume and open

[40] To remove highly illiquid contracts, for SPX and NDX we keep only options with standardized moneyness, defined as $m = \ln(K/S)/(IV_{ATM}\sqrt{\tau})$, between -10 and 5 and Black-Scholes implied volatility less than 1. For AMZN only, we keep options with Black-Scholes delta between 0.01 and 0.99 (in absolute value) given the highly illiquid contracts beyond that range.

Table 1: **Summary Statistics for Put and Call Options**: The sample size is 1,258 for both puts and calls. First five columns report put statistics and second five columns report call statistics. Moneyness (normalized) are OTMmin = $log(K_{min}/S)/(\sigma_{ATM}\sqrt{\tau})$, ITMmax = $log(K_{max}/S)/(\sigma_{ATM}\sqrt{\tau})$. K_{min} is out-of-the-money (OTM) for puts and in-the-money (ITM) for calls. K_{max} is ITM for puts and OTM for calls. $N^p|N^c$ are the number of put/call options. Volume and Open Interest (reported as $\times 1000$) are sums of all the volume and open interests across all strikes between K_{min} and K_{max} of the maturity (in days) with highest volume. Bid-Ask-Spread shows the average bid-ask spread of option prices as a percentage of the option mid-point. Panels A, B, C, D correspond to SPX, NDX, AMZN, and FB, respectively.

	Puts					Calls				
	Mean	SD	P25	P50	P75	Mean	SD	P25	P50	P75
Panel A: SPX										
OTMmin	-9.66	0.35	-9.84	-9.75	-9.59	-6.65	2.83	-9.56	-7.08	-3.86
ITMmax	2.61	1.38	1.33	2.25	3.99	3.24	0.75	2.66	3.13	3.81
$N^p\|N^c$	132.86	45.84	99	130	164	110.77	45.82	77	105	138
Volume	127.7	63.7	83.97	113.21	154.72	74.37	40.6	45.02	66.59	94.13
Open Interest	1255.37	663.76	772.87	1116.27	1833.27	824.39	526.25	421.25	618.23	1289.96
Maturity	23.11	12.06	11	23	32	23.11	12.06	11	23	32
Bid-Ask Spread	0.33	0.19	0.17	0.33	0.48	0.20	0.09	0.14	0.18	0.24
ATM IV	0.12	0.04	0.09	0.11	0.14	0.12	0.04	0.09	0.11	0.14
Panel B: NDX										
OTMmin	-8.33	1.53	-9.43	-8.96	-7.63	-5.87	2.8	-8.92	-5.75	-3.14
ITMmax	2.25	1.26	1.24	1.67	3.23	2.73	0.87	2.03	2.59	3.26
$N^p\|N^c$	119.9	49.73	86	111	140	110.1	46.92	78	104	137
Volume	5.18	8.92	1.98	3.09	5.19	2.32	2.91	0.8	1.46	2.64
Open Interest	28.15	28.65	9.49	18.14	36.14	16.71	15.3	3.84	11.81	25.37
Maturity	18.12	9.88	9	16	25	18.12	9.88	9	16	25
Bid-Ask Spread	0.32	0.18	0.20	0.28	0.43	0.18	0.11	0.10	0.16	0.23
ATM IV	0.16	0.05	0.12	0.14	0.17	0.16	0.05	0.12	0.14	0.17
Panel C: AMZN										
OTMmin	-4.05	0.8	-4.55	-4.03	-3.52	-4.92	2.71	-6.8	-4.34	-2.64
ITMmax	4.31	2.85	1.82	3.49	6.29	2.96	0.66	2.51	2.85	3.3
$N^p\|N^c$	89.61	56.87	48	73	113	87.41	57.25	47	71	109
Volume	8.68	5.71	4.77	7.16	10.78	10.45	7.54	5.51	8.57	12.95
Open Interest	30.85	18.87	14.4	29.1	41.34	34.76	22.94	15.09	32.63	47.01
Maturity	15.27	8.93	8	11	23	15.27	8.93	8	11	23
Bid-Ask Spread	0.13	0.08	0.07	0.11	0.18	0.14	0.08	0.08	0.12	0.17
ATM IV	0.28	0.11	0.20	0.25	0.32	0.28	0.11	0.21	0.25	0.32
Panel D: FB										
OTMmin	-5.45	1.87	-6.43	-5.13	-4.11	-6.33	3.65	-8.62	-5.72	-3.17
ITMmax	5.26	3.72	1.83	4.34	7.82	3.32	1.06	2.56	3.12	3.9
$N^p\|N^c$	36.61	15.42	25.25	35	44	34.34	14.88	24	32	41
Volume	22.86	16.22	12.69	18.37	27.55	38.49	27.22	20.77	31.57	46.91
Open Interest	132.38	86.23	52.65	127.64	184.41	210.68	137.18	86.51	210.93	283.97
Maturity	17.1	10.18	8	15	24	17.1	10.18	8	15	24
Bid-Ask Spread	0.16	0.08	0.11	0.15	0.20	0.11	0.06	0.07	0.11	0.14
ATM IV	0.28	0.11	0.20	0.25	0.33	0.28	0.11	0.20	0.25	0.33

interest.

Regarding the underlying assets, our data sources differ between individual stocks and indexes. Since equity options and their corresponding underlying assets (AMZN and FB) trade in a synchronized fashion with both the option and equity markets closing at 4:00 p.m. EST, we use the closing prices provided by OptionMetrics. For indexes (SPX and NDX), the option market closes at 4:15 p.m. while the cash market closes at 4:00 pm. Even though OptionMetrics collects option quotes as closely as possible to 4:00 p.m., in order to avoid potential issues of asynchronous prices[41] we follow Andersen et al. (2015) and use put-call parity[42] to compute the *implied price* of the underlying index. More specifically, because options on SPX and NDX are European-style, we use the relation $F_{t,\tau} = K + e^{r\tau}(C_t(K,\tau) - P_t(K,\tau))$ to compute the implied forward price $F_{t,\tau}$ for a common set of strikes K across put and call options pairs with the same maturity τ. We then take the median $F_{t,\tau}$ using the five option contracts that are closest to at-the-money because they tend to be the most liquid, making it more likely put-call parity is satisfied. Finally, using the risk-free rate (obtained by linearly interpolating the zero-yield curve provided by OptionMetrics to match the option maturity) and the continuously compounded dividend yield (provided by OptionMetrics), we compute the implied spot price as $S_t = F_{t,\tau}e^{(r_t-\delta_t)\tau}$.

5 The Empirical Analysis

This section discusses the estimation of the G-SVJD model and call option bubbles for the four assets analyzed in our main empirical study: SPX, NDX, AMZN, and FB.

5.1 The G-SVJD Model Estimation

Table 2 shows the summary statistics for the daily estimated parameters of the G-SVJD model, their median standard errors[43] (computed following the infill asymptotic theory developed in Andersen et al. (2015)) and the $RMSE_{IV}$. The average parameter estimates are quite similar across the assets, with a few exceptions. The equity index volatilities, on average, are between 10% and 13%, while AMZN and FB display much larger values of around

[41] See IvyDB US Reference Manual v4.0, p. 19.

[42] Of course, this is consistent with our maintained assumptions of NFLVR and ND.

[43] The infill asymptotic theory in Andersen et al. (2015) relies on a fixed-time span and a growing number of option in the cross section (i.e. on a given day and for a given maturity). While these assumptions are certainly satisfied by SPX and NDX, for AMZN and FB, where the number of available options is significantly smaller, the small-sample standard errors would be much larger than the asymptotic ones reported in Table 2.

30%. This is consistent with the fact that the ATM IV (as reported in Table 1) is much higher for equity than for index options. All assets have similar average negative jump sizes, with the single stocks' jump intensities being twice as large as those of SPX and NDX.

The correlation coefficient ρ is negative, on average, for all the assets, but less so for AMZN and FB. It is important to notice that while ρ is tightly estimated in the case of SPX and NDX, it is estimated with large standard errors in the case of AMZN and FB. The parameter p is generally estimated with high precision and it is equal to approximately 0.2 for indexes and 0.35 for single stocks. Both values are significantly smaller than the value of 0.5 which is commonly used in the option-pricing literature, pointing to the fact that the affine specification for the variance process seem to be rejected when confronted with option data.

Despite the large standard errors of the individual parameter estimates as discussed above, in terms of the option-pricing fit, the G-SVJD model does a remarkable job in pricing put options. The average $RMSE_{IV}$ is 0.57% and 0.49% for SPX and NDX, respectively. These are small percentage errors which are similar to the best performing model in Andersen et al. (2017), especially when considering that the P99 is around 1.4%. The $RMSE_{IV}$ for AMZN and FB are larger, 0.95% and 1.17%, respectively. This result needs to be interpreted while recognizing that the equity option implied volatilities are much larger (almost eightfold) than those of the index options (see Table 1). Nevertheless, more than 50% of the days have a $RMSE_{IV}$ of less than 1% and the 75th percentile is also close to 1%.

This documented difference between the noisy asset price parameter estimates, in contrast to the accuracy of the estimated option prices, is our primary motivation for using option data (as opposed to time series asset price data) to test for the existence of asset price bubbles. As a robustness test of our results, after presenting the call option bubble estimates, we revisit the evidence with respect to the existence of bubbles based on the parameter estimates alone.

5.2 The Option Bubble Estimation

In this section we analyze the daily call option bubble estimates. We first describe the results for the equity indexes (SPX and NDX) and then for the individual stocks (AMZN and FB).[44]

[44]When presenting the time-series plot, coherently with our framework, we report only the estimated positive bubble because, as described in Section 3, negative values reflect estimation error and market microstructure noise. The average size of the negative bubble is, of course, reflected in the time-varying threshold used in the conditional test described in Section 3.4 and depicted with a red dotted line in Figure 5. Also, in order to reduce the impact of noisy data and to reduce concern about model mispecification, we exclude from our analysis the days with the 5% of highest $RMSE_{IV}$ for all the assets (these are the days in which the G-SVJ model has the poorest fit).

Table 2: **G-SVJD Model Estimation Results**: This table reports the means, standard deviations (SD), the 1st (P01), 25th (P25), 50th (P50), 75th (P75), 99th (P99) percentiles of the daily parameter estimates and the $RMSE_{IV}$ (%), as well as the corresponding median of the daily standard errors. Panels A, B, C, D correspond to SPX, NDX, AMZN, and FB, respectively.

	Mean	SD	P01	P25	P50	P75	P99	StdErr
Panel A: SPX								
V_0	0.011	0.013	0	0.003	0.007	0.013	0.064	0.004
σ_V	0.322	0.148	0.07	0.229	0.296	0.396	0.773	0.070
ρ	-0.805	0.176	-0.99	-0.933	-0.839	-0.724	-0.305	0.048
p	0.205	0.138	0.1	0.132	0.189	0.243	0.47	0.002
μ_y	-0.219	0.18	-0.791	-0.296	-0.177	-0.1	0.102	0.028
σ_y	0.229	0.179	0.003	0.119	0.179	0.277	0.91	0.027
λ	0.135	0.208	0.007	0.036	0.079	0.156	0.888	0.002
$RMSE_{IV}(\%)$	0.57	0.28	0.18	0.38	0.52	0.70	1.47	
Panel B: NDX								
V_0	0.019	0.02	0	0.007	0.013	0.022	0.103	0.006
σ_V	0.398	0.178	0.071	0.289	0.372	0.469	0.956	0.100
ρ	-0.717	0.194	-0.989	-0.836	-0.744	-0.634	-0.19	0.051
p	0.189	0.16	0.1	0.114	0.155	0.211	0.642	0.002
μ_y	-0.221	0.19	-0.787	-0.3	-0.177	-0.09	0.11	0.045
σ_y	0.238	0.22	0.001	0.101	0.16	0.273	0.982	0.045
λ	0.176	0.324	0.007	0.039	0.083	0.188	1.666	0.004
$RMSE_{IV}(\%)$	0.49	0.24	0.13	0.32	0.44	0.59	1.35	
Panel C: AMZN								
V_0	0.079	0.074	0.004	0.035	0.055	0.091	0.381	0.008
σ_V	0.586	0.321	0.047	0.358	0.546	0.754	1.6	0.502
ρ	-0.578	0.374	-0.99	-0.889	-0.615	-0.381	0.864	0.133
p	0.4	0.396	0.1	0.13	0.251	0.509	1.939	0.010
μ_y	-0.213	0.284	-0.798	-0.379	-0.192	-0.051	0.7	0.256
σ_y	0.53	0.346	0.001	0.172	0.549	0.874	1	0.247
λ	0.241	0.52	0.003	0.044	0.082	0.177	2.886	0.008
$RMSE_{IV}(\%)$	0.95	0.62	0.21	0.50	0.78	1.21	2.99	
Panel D: FB								
V_0	0.08	0.084	0.001	0.033	0.057	0.096	0.404	0.021
σ_V	0.646	0.313	0.114	0.438	0.591	0.805	1.599	0.545
ρ	-0.613	0.327	-0.99	-0.881	-0.637	-0.447	0.818	0.170
p	0.327	0.339	0.1	0.122	0.195	0.394	1.815	0.011
μ_y	-0.157	0.306	-0.794	-0.352	-0.135	0.024	0.69	0.255
σ_y	0.551	0.339	0.001	0.224	0.58	0.884	1	0.213
λ	0.249	0.61	0.004	0.032	0.065	0.165	3.647	0.005
$RMSE_{IV}(\%)$	1.17	0.86	0.20	0.63	0.94	1.40	4.53	

Because our estimation is done day-by-day using only one option cross-section per day, and with the number of available options changing over time, the estimation results are subject to noise. As a result, interesting periods are those characterized by a *persistent* sequence of estimated positive bubbles rather than days with *isolated* positive bubbles.

For each asset, Figure 5 shows on the right axes the daily asset price (solid lines, green color) and on the left axes the estimated call option bubble magnitudes as a percentage of stock prices, $\hat{\mathbb{B}}_t$, (dashed lines, blue color) and the time-varying critical values that corresponds to the statistical test described in Section 3.4 for a one-side probability of 10%, i.e. we define a time varying threshold as $\mathbb{T}_t = 1.65\hat{\sigma}_t$.[45] We estimate the volatility of the error, σ_t, on each day, using the estimated negative bubbles, $\hat{\mathbb{B}}_t$, over the previous 180 days as described in Section 3.4. This implies that, at each time t, the call option bubble can be considered statistically significant whenever it exceeds the threshold $\mathbb{T}_t$.[46] And, under the assumption of ND, this implies that the underlying asset exhibits a statistically significant price bubble as well. It is important to mention that if ND, or equivalently, put-call parity is violated, the call option bubble estimates and significance are unaffected. It is only the linear relation between the underlying asset's price bubble and the call option's bubble that will contain some error.[47]

From Panels (a) and (b) of Figure 5 we notice that call option bubbles in both the SPX and NDX often lie in a tight range above zero, with occasional isolated spikes. We observe a different behavior in Panels (c) and (d) of Figure 5 for AMZN and FB. For both stocks the estimated call option bubbles are in the vicinity of zero most of the time, but they also show periods with *clusters* of large significant bubbles, in particular at the beginning of 2016 and at the beginning and at the end of 2018. The estimated call option bubbles for AMZN and FB are both more frequent and larger in magnitude than the bubbles estimated for both SPX and NDX. This finding can be explained by the fact that because indexes are weighted averages of their constituent stocks, the corresponding asset price bubble reflects the "average bubble" among its constituents, which will be much smaller and more stable over time relative to bubbles in single stocks. And, this is reflected in lower magnitudes for the call option bubbles on the indexes versus the individual equities. Recall that call option bubbles provide a lower bound on the underlying asset's price bubble as depicted in

[45] In order to reduce the impact outliers we estimate σ_t via $\left(\sqrt{median(\hat{\sigma}^2_{N_-})}\frac{3}{2}\right)$ which is theoretically consistent with the assumption of a normal distribution for the error term ε_t.

[46] Changing the probability level to 5% or 1% leads to quantitatively similar results.

[47] This same statement applies to violations of put-call parity due to various market frictions, including security lending fees (or short sale costs).

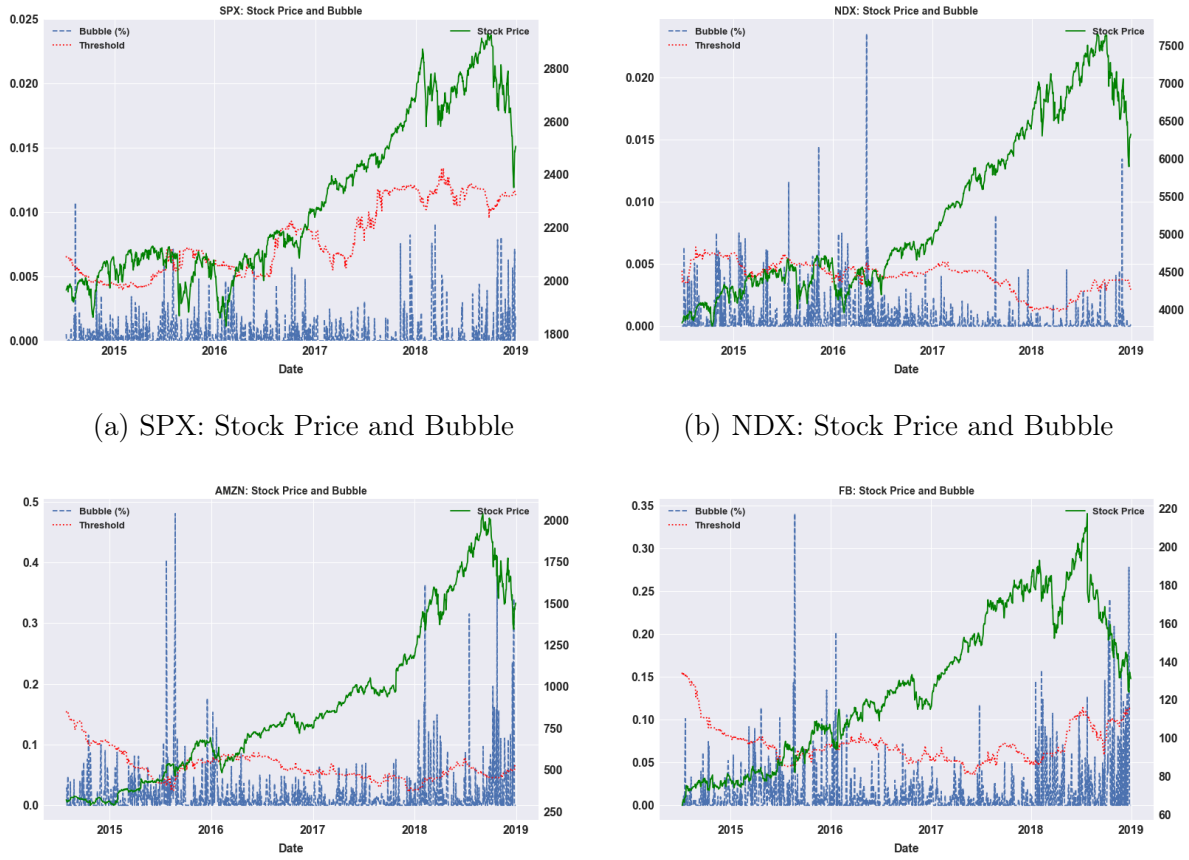

(a) SPX: Stock Price and Bubble

(b) NDX: Stock Price and Bubble

(c) AMZN: Stock Price and Bubble

(d) FB: Stock Price and Bubble

Figure 5: **SPX, NDX, AMZN, and FB: Stock Prices and Bubbles**. Panels (a), (b), (c) and (d) show on the right axes the stock prices (solid lines, green color) and the left axes the estimated bubble magnitudes as a percentage of stock prices (dashed lines, blue color). Each Panel also shows the time-varying threshold $\mathbb{T}_t = 1.65\hat{\sigma}_t$ (dotted lines, red color).

expressions (6) and (8).[48]

In order to illustrate how our call option bubble estimates hinge on the differential pricing between put and call options, in Figure 6 we report the results on two representative days for AMZN and FB. Although our call option bubble estimates depend on the difference between option prices, we graph implied volatilities (which are non-linear functions of option prices) as they allow one to better visualize the gap between market and model call prices. On both days the estimated call option bubble is positive and significant. This implies, of course, that there exists a bubble in the underlying asset. As can be seen in the left panels, on

[48]For all four assets, the patterns in the call option bubble estimates reported in Figure 5 remain qualitatively and quantitatively similar when we compute bubbles as in Equation (20) using only ITM or OTM options, or when using only call options with positive trading volume.

both days and for both assets, the fit of the G-SVJ model on the put options is extremely accurate, with a $RMSE_{IV}$ for AMZN equal to 1.5% and 0.8% for FB. For the same days, the right panels show the observed implied volatility of the call options along with the implied volatility generated by the G-SVJ model based on the parameter estimates obtained by fitting the model to put options. It is evident that there is a large and persistent (in the moneyness dimension) gap between the two lines. Intuitively, our call option bubble estimate is proportional to the area between the market observed call's implied volatility and the model implied volatility.[49]

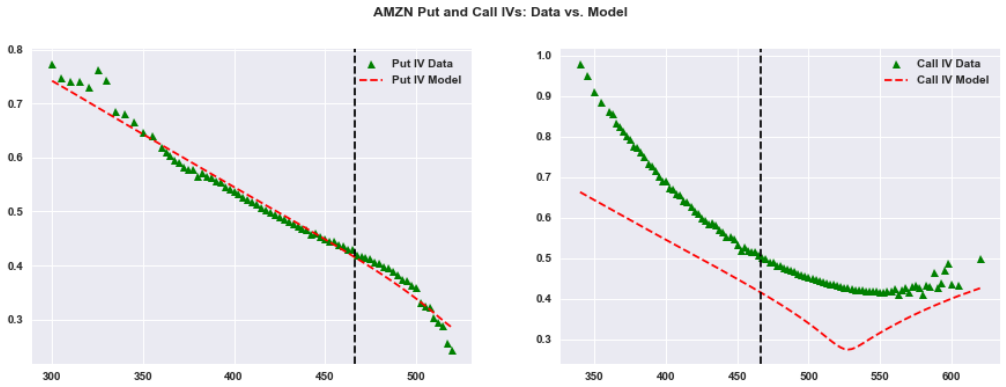

(a) AMZN: August 25, 2015

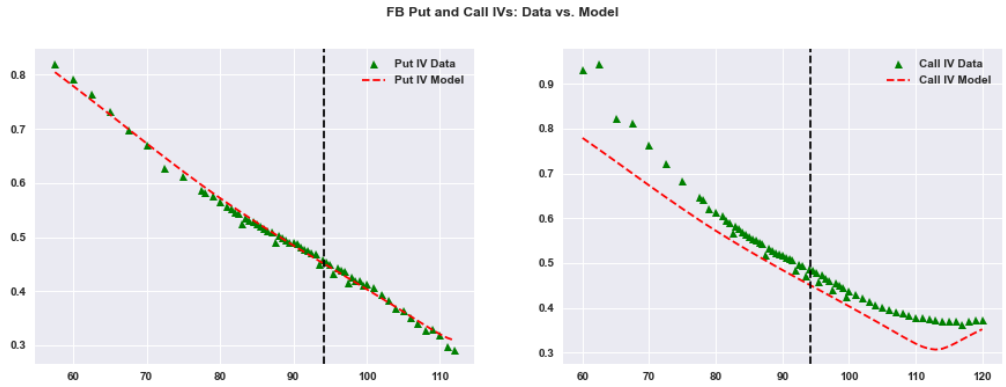

(b) FB: January 21, 2016

Figure 6: **AMZN and FB: Puts, Calls, and Bubbles**. The figure shows in the left (right) panels, the observed implied volatility of put (call) options, green triangles, and the implied volatility generated by the G-SVJ, red dashed line. Panel (a) corresponds to Amazon on August 25, 2015 (24 days-to-maturity). The $RMSE_{IV}$ in pricing the put options is equal to 1.5%. Panel (b) corresponds to Facebook on January 21, 2016 (29 days-to-maturity. and $RMSE_{IV}$ in pricing the put options is equal to 0.7%.

[49]Recall from Equation (19) that when the call's market price is higher (lower) than the model call's price the estimated bubble is positive (negative).

The formal results of the statistical test for non-zero call option bubbles are reported in the Table 3. The first row shows that while SPX and NDX have very rare bubble episodes, with a frequency of less than 1% over the entire sample, AMZN and FB display a larger number of significant call option bubble instances which are identified in around 5%-8% of the days. The bottom Panel of Table 3 reports the average $RMSE_{IV}$ option over the entire sample and over days with negative, positive, and significantly positive call option bubbles. It is important to emphasize that this statistical test, under our assumption of ND, is also a statistical test for the existence of price bubbles in the underlying asset. The key difference is that the magnitude of the option bubble measured here is smaller than the magnitude of the asset price bubble, although the two are linearly related.

As seen from Figure 5, the only significant SPX asset price bubble episodes are in 2014. NDX experienced slightly more instances of positive asset price bubbles relative to SPX with relatively larger magnitudes as reflected in the call option bubbles. However, the few significant asset price bubbles in both indexes tend to be isolated. The latter fact, coupled with the observation that days with estimated positive bubbles also tend to have larger pricing errors than the average over the full sample (0.7% and 0.5% versus 0.51% and 0.44%, respectively), indicates that those few episodes should be considered with caution. In contrast, single stocks experience much more frequent and larger asset price bubbles as reflected in call option bubbles. Also, Table 3 shows that on days in which we detect a call option bubble (for both AMZN and FB), the $RMSE_{IV}$ is actually significantly smaller (0.68% and 0.71%) than the average $RMSE_{IV}$ over the entire sample (0.80% and 0.99%). Importantly, the $RMSE_{IV}$ for days with negative call option bubbles is higher than the average $RMSE_{IV}$. This provides evidence consistent with our assumption that days with negative bubbles are affected by estimation noise.

As for the call option bubble's magnitude, AMZN's bubble ranged between 10 and over 20 bps from mid-2015 to early 2016, followed by numerous instance of over 10 bps spread over the course of 2018. FB's call option bubble ranged above 10 bps from mid-2015 to early 2016, followed by numerous instances of over 15 bps in 2018.[50] In terms of dollars, the average call option bubbles above 20 bps for AMZN in 2018 imply a bubble of ≈\$5.5. Then, given that each option contract is written on 100 shares this in fact imply ≈ a \$550 call option bubble. Similarly, the average of the call option bubbles above 15 bps for FB in

[50]The overall call option bubble patterns as discussed above and as shown in Figure 5 are robust to bubbles computed over different delta ranges (e.g. deltas from 1 to 0.4 that mostly capture ITM options or deltas from 0 to 0.6 that mostly capture OTM options), pointing to the fact that, as theory suggests, the estimated option bubbles do not depend from the option's strike price.

Table 3: **Statistical Tests**. The first row reports the percentages of days in which the null hypothesis of the statistical test in Section 3.4 (i.e. $\mathbb{B}_t = 0$) is rejected with a one-side probability of 10%. The second, third, fourth, and fifth rows report the average $RMSE_{IV}$ (i) over the entire sample period, (ii) on days when $\hat{\mathbb{B}}_t < 0$, (iii) on days when $\hat{\mathbb{B}}_t > 0$, and (iv) on days when the null is rejected, respectively. The sample size is equal to 1076 (there is a burn-in period of 180 days needed to compute the first estimate of the variance of ε_t dropping 5% of highest $RMSE_{IV}$ observations).

	SPX	NDX	AMZN	FB
% of days above threshold	0.37	3.43	8.00	5.48
	$RMSE_{IV}$(%)			
Entire Sample	0.51	0.44	**0.80**	**0.99**
Negative Bubbles	0.52	0.46	0.98	1.24
Positive Bubbles	0.50	0.43	0.66	0.76
Bubble Above Threshold	0.74	0.58	**0.68**	**0.71**

2018 imply an average bubble magnitude of $\approx$ \$0.35 for a total of $\approx$ \$35.

As explained in Section 2.2, the call option magnitudes reported above reflect the amount of the asset price bubble that is embedded into the option contracts of a given maturity. Because the model horizon T is larger than the maturity of the option, the full size of the asset price bubble can be orders of magnitude larger (see for example, the simulation study in Appendix C).

To summarize, our evidence points to the presence of short-lived but persistent call option bubble episodes in both AMZN and FB, over the 2014–2018 implying the existence of asset price bubbles in the underlying stocks. In contrast, the stock indexes SPX and NDX do not show periods of persistent call option bubbles, implying less frequent asset price bubbles in the indexes themselves. In the next sections we focus on AMZN and FB and we investigate potential economic channels that can explain the presence of bubbles in those assets.

5.3 Implications of Price Bubbles

Given the above evidence about the presence of short-lived and persistent price bubbles in AMZN and FB, in this section we discuss some economic implications of the estimated bubbles. We do so by analyzing four issues that are often associated with price bubbles: volatility, trading volume, earning announcements, and rapid price increases (or price bursts).

The volatility of the underlying asset plays a prominent role in the detection of bubbles because the explosive behavior of volatility (relative to the drift) determines whether a price

bubble exists. Our estimation results can be used to highlight the time-series relationship between price bubbles and volatility. Indeed, the underlying *priced* volatility can be measured by the expectation of its risk-neutral quadratic variation:

$$\begin{aligned} QV_{[t,t+\tau]} &= \tfrac{1}{\tau} E_t \left[\int_t^{t+\tau} V_s ds + \textstyle\sum_{t<s\leq t+\tau} \Delta J_s^2 \right] \\ &\approx V_{0,t} + 2\lambda_t (e^{\mu_{y,t}+0.5\sigma_{y,t}^2} - \mu_{y,t} - 1), \end{aligned} \tag{22}$$

where the approximation relies on the fact that volatility tends to be highly persistent so that the integral and sum can be approximated by the spot variances. Figure 7 documents a large positive correlation between the estimated call option bubbles and the underlying quadratic variation. The correlation coefficient is equal to 0.58 for AMZN and 0.55 for FB.

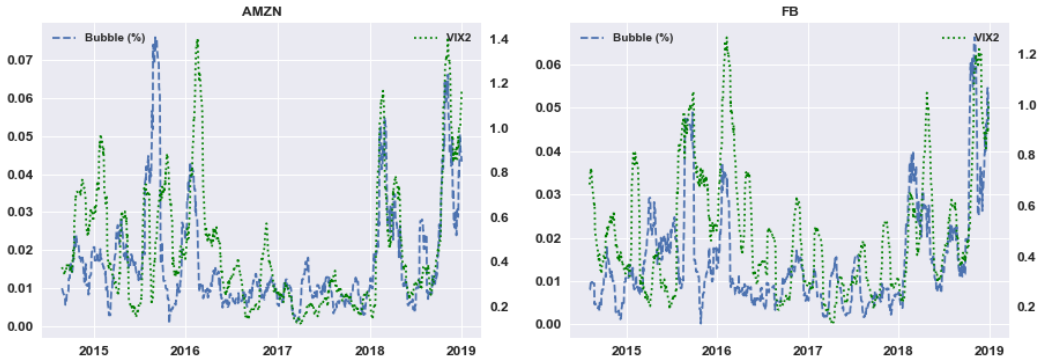

Figure 7: **Option Bubbles and Quadratic Variation**. The figure shows the time series of the smoothed (21-day backward looking moving average) positive call option bubble estimates (blue-line) and estimated quadratic variation (green-line) for AMZN (left panel) and FB (right panel).

Second, it is reasonable to believe that periods marked by pronounced price bubbles are also characterized by increased trading activity. The intuition is that higher trading volume is generally associated with increased volatility and that, as volatility increases, the asset price process is more likely to exhibit a large bubble.[51] To investigate the relationship between price bubbles and volume we estimated the following regression:

$$\hat{\mathbb{B}}_t^+ = \nu_0 + \nu_1 \times \ln(\text{Volume}_t) + \epsilon_t, \tag{23}$$

where $\hat{\mathbb{B}}_t^+$ refers to instances of the positive call option bubbles and $\ln(\text{Volume}_t)$ is the natural logarithm of the daily traded volume of the underlying asset (so that we can interpret the

[51] This intuition is based, for example, on the fact that in a simple diffusive model for the stock price a bubble exists if and only if $\int_\varepsilon^\infty \frac{s}{\sigma^2(s)} ds < 0$, for some $\varepsilon > 0$ (see Delbaen and Shirakawa (2002)).

Table 4: **Call Option Bubble Magnitude and Trading Volume:** This table reports the results for the regression of the estimated positive call option bubbles on the trading volume of the underling asset. t-values are reported in parentheses. Coefficient estimates are reported as percents (%).

	AMZN	FB
Intercept	-0.3301	-0.1589
	(-8.28)	(-4.69)
Ln(Volume)	0.0230	0.0102
	(8.72)	(5.12)
R^2	0.06	0.02

coefficient ν_1 as the effect on the bubble magnitude of a one percentage increase in the volume).

Table 4 shows the regression results for Equation (23). In particular, the coefficient ν_1 is positive and statistically significant for all four assets. A one percent increase in trading volume leads to an increase of about 0.0230%, and 0.0102% in the call option's bubble magnitude for AMZN and FB, respectively. Not surprisingly the larger coefficient for AMZN is consistent with previous results showing that AMZN has the highest frequency of large and significant bubbles.

Third, even though there could be numerous (and potentially unpredictable) factors that prompt the occurrence of a bubble, earnings announcements are of particular interest. These events are scheduled in advance and trading in both options and the underlying assets before earnings announcement days could be driven by expectations about price reactions to an announcement. In essence, earnings announcements allow us to directly test for an important instance of the buy-to-resell motive behind the bubble. We do so by running the following regression for AMZN and FB:

$$\hat{\mathbb{B}}_t^+ = \eta_0 + \eta_1 \times Dum_{1-14} + \eta_2 \times Dum_{15-28} + \eta_3 \times Dum_{29-42} + \epsilon_t, \tag{24}$$

where we define a dummy variable $Dum_{t_1-t_2} = 1$ if an earnings announcement is scheduled between time $t+t_1$ and $t+t_2$ and zero otherwise. The results of the regression are reported in the first and third columns of Table 5 (denoted by AMZN (1) and FB (1)). As seen, for both AMZN and FB the coefficients of the first and the second dummy variables $Dum_{1,14}$ and $Dum_{15,28}$, respectively, are positive and the first variable is particularly significant. Interestingly, the dummy variable coefficients are decreasing in general for both stocks, suggesting

Table 5: **Call Option Bubbles and Earning Announcements**: This table reports the results for the regression of the estimated positive call option bubbles on a sequence of dummy variables that identify the number of days before an earning announcement. In particular, $Dum_{t_1-t_2} = 1$ if an earnings announcement is scheduled between time $t+t_1$ and $t+t_2$. t-statistics are reported in parentheses. Coefficient estimates are reported as percents (%).

	AMZN (1)	AMZN (2)	FB (1)	FB (2)
Intercept	0.0151	-0.3258	0.0116	-0.1362
	(7.51)	(-7.92)	(8.17)	(-4.27)
Dum_{1-14}	0.0056	0.0063	0.0078	0.0072
	(1.74)	(2.00)	(3.27)	(3.06)
Dum_{15-28}	0.0020	0.0045	0.0046	0.0049
	(0.61)	(1.43)	(1.89)	(2.06)
Dum_{29-42}	-0.0016	0.0025	-0.0022	-0.0010
	(-0.50)	(0.77)	(-0.91)	(-0.43)
Ln(Volume)		0.0224		0.0087
		(8.30)		(4.64)
R^2	0.01	0.07	0.02	0.04

that, all else equal, the closer the earnings announcement date the larger the estimated call price bubble, and by implication the underlying asset price bubble. Finally, the second and fourth columns of Table 5 (denoted by AMZN (2) and FB (2)), show that the effect of earnings announcements is robust to the inclusion of volume as a control.

Fourth, there is a widespread tendency to identify a period marked by a rapid asset price increase (or price burst) with the manifestation of a bubble. However, our framework and results show that rapid price increases do not necessarily imply the existence of a bubble. For example, from early 2016 to late 2017, FB's market price increased from around \$100 to nearly \$200, almost a 100% price increase. Similarly, AMZN's price increased from \$500 in early 2016 to around \$1200 by late 2017, exceeding a 140% increase. However, we did not find many significant call option bubbles during this period, implying that there are no stock price bubbles. Similarly, NDX increased from around \$4000 in early 2016 to over \$7500 by mid-2018 (almost a 100% increase). SPX increased from around \$1800 to over \$2800 by mid 2018 (an increase in excess of 50%). Again, our estimates show no significant

call option bubbles during this period, implying that there are no index price bubbles. What matters for the occurrence of a bubble is the market's forward-looking expectations regarding company-specific and/or market-wide fundamentals and the future resale value of the asset. Our analysis shows that option prices, which are driven by investors' forward-looking expectations, can be effectively used to estimate price bubbles in underlying assets.

5.4 Stock Price Parameters and Bubbles

In this section we analyze the relationship between the estimated call option bubbles and the parameters of the underlying G-SVJD process. Given the limited sample and the small number of significant call option bubbles across the four assets, in order identify reliable patterns in the data we focus on time-series averages of the estimated call option bubbles and parameters ρ and p.[52]

Figures 8 and 9 show the time-series of the estimated parameters p and ρ. Also, Table 2 reports summary statistics of the parameters' distribution and the median of the standard errors. A few observations are in order. First, while a large majority of option pricing models assumes both the correlation coefficient ρ and the variance's exponent in the volatility of volatility p to be constant, our empirical evidence points to a significant time variation of these parameters. Second, as can be seen from Figures 8 and 9, while ρ and p are accurately estimated in the case of SPX and NDX, they are estimated with large standard errors (especially ρ) in case of AMZN and FB. Third, as reported in Table 6, ρ and p are highly positively correlated, with the correlation coefficient ranging from 0.5 for FB to 0.62 for SPX. When we pool all the assets together as described in the previous paragraph, the overall correlation is equal to 0.64 (last column of Table 6). It is important to notice that our estimation procedure does not force any ex-ante relationship between ρ and p. Hence, the evidence presented here suggests that the parameters governing the existence (or lack of) of a bubble have a tight empirical relationship.

One's first thought is to investigate whether days in which we estimate positive call option bubbles also see ρ_t and p_t lying in the appropriate region of the parameter space. Recall that, according to our theoretical framework, a bubble exists in the underlying asset if and only if $\rho > 0$ and $0.5 < p < 1.5$ (see Figure 2). This provides a robustness check of our methodology and the ND assumption.[53] The problem with this robustness check, however, is that our

[52] Using a time-series average strikes a balance between controlling for negative bubble instances which are averaged out and producing a less noisy time-series bubble estimate, which reveals more stable relationships in the cross section of bubble and parameter estimates.

[53] Recall that call option bubbles can exist even when the stock price has none. They are linearly related

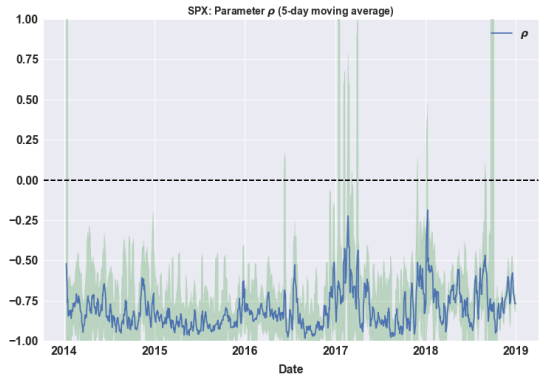

(a) SPX: Parameter ρ

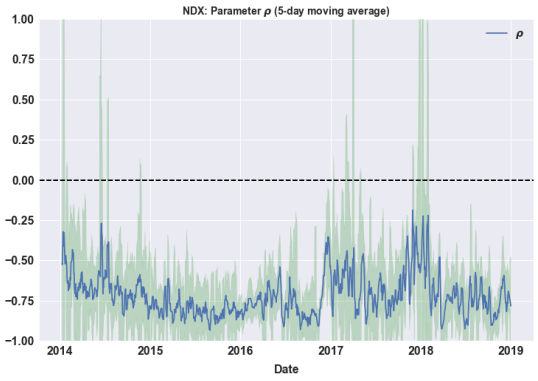

(b) NDX: Parameter ρ

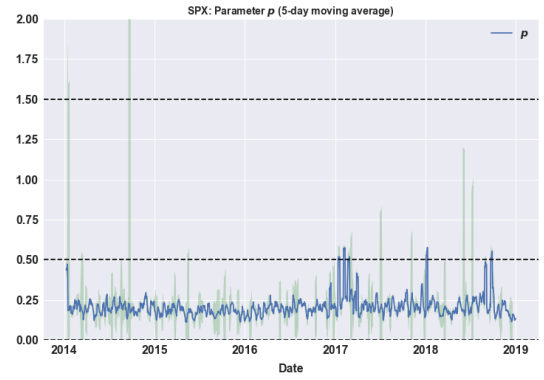

(c) SPX: Parameter p

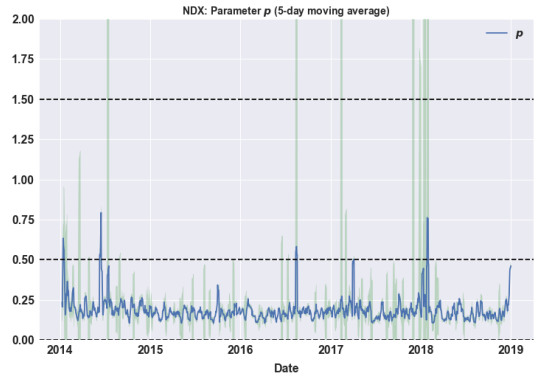

(d) NDX: Parameter p

Figure 8: **SPX and NDX Parameter Estimates**. Panels (a), (b), (c), and (d) show the the 5-day time-series moving average of the estimated parameters ρ (Panels (a) and (b)) and p (Panels (c) and (d)) .

parameter estimates have large standard errors, making statistical tests of this set inclusion unreliable. Nonetheless, performing some comparative analyses based on these parameter estimates still provides some useful insights into the validity of our methodology. We focus on the overall patterns between the parameter estimates and the call option's bubble in order to determine whether they are reasonably consistent with the theory, thereby providing an indirect test of the ND assumption (and put-call parity).[54]

We do this by pooling together, across assets, the 21-day moving averages of the estimated bubbles and parameters.[55] We then run the following OLS and logit regressions, which are

if ND holds.

[54]This is analogous to the use of an analyst's earnings forecast for determining a company's profitability. The magnitude of the forecast, due to its large error, is often less revealing than the time series patterns of the forecasts for determining a company's profitability.

[55]Given the noisy short-term parameter estimates, as seen with 5-day moving averages in Figures 8 and 9,

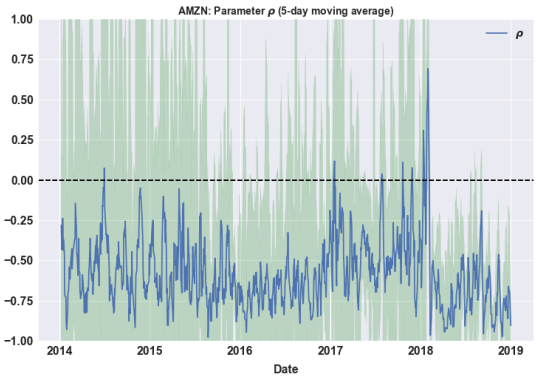

(a) AMZN: Parameter ρ

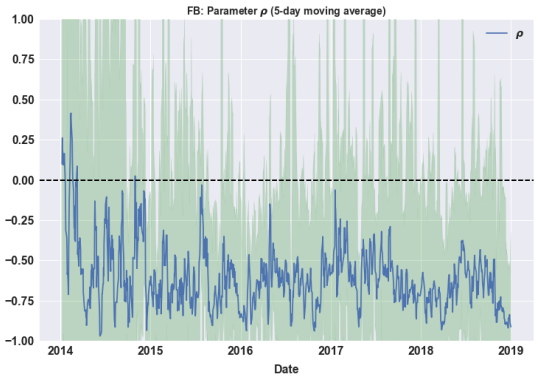

(b) FB: Parameters ρ

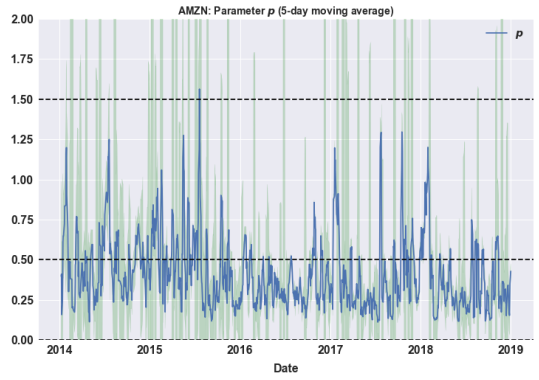

(c) AMZN: Parameter p

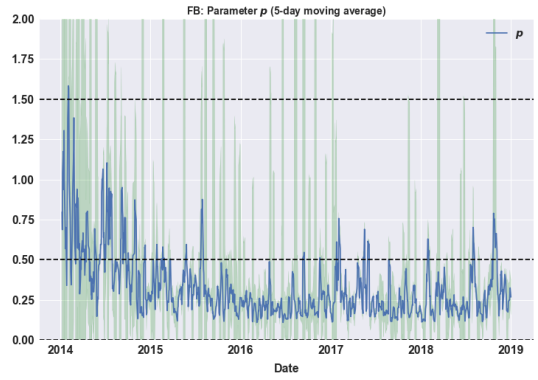

(d) FB: Parameter p

Figure 9: **AMZNand FB Parameter Estimates**. Panels (a), (b), (c), and (d) show the the 5-day time-series moving average of the estimated parameters ρ (Panels (a) and (b)) and p (Panels (c) and (d)) .

meant to capture the relationship between the parameters ρ and p and both the call option bubble's *magnitude* and the *probability* of it occurring.

$$\hat{\mathbb{B}}^{+}_{t,i} = \beta_0 + \beta_1 \times \rho_{t,i} + \beta_2 \times Dum_{p,t,i} + \beta_3 \times (Dum_{p,t,i} \times \rho_{t,i}) + \epsilon_{t,i} \tag{25}$$

$$\text{Logit}(1_{\{\hat{\mathbb{B}}_{t,i} \geq 0\}}) = \beta_0 + \beta_1 \times \rho_{t,i} + \beta_2 \times Dum_{p,t,i} + \beta_3 \times (Dum_{p,t,i} \times \rho_{t,i}) + \epsilon_{t,i} \tag{26}$$

where $i \in \{SPX, NDX, AMZN, FB\}$, $Dum_{p,t,i} = 1$ whenever $0.5 < p_{t,i} < 1.5$ and zero otherwise. $Dum_{p,t,i} \times \rho_{t,i}$ is an interaction term that captures the non-linear relation between the parameters and the call option bubble.

Table 7 reports the pooled OLS and logit regression estimates for the pooled data, along

we choose 21-day moving averages to pool into one cross-section to focus on the general patterns as previously discussed.

Table 6: **Correlation**: The table reports the correlation between ρ and p for all four assets (SPX, NDX, AMZN, and FB) and the pooled assets (All).

	SPX	NDX	AMZN	FB	All
$Corr(\rho_t, p_t)$	0.62	0.55	0.52	0.50	0.64

Table 7: **OLS and Logit Regressions of Bubble on Parameters**: This table reports the coefficients of the OLS regression (25) and logistic regression (26) with t-statistics in parentheses. Coefficient estimates of OLS regression are reported as percents (%).

	OLS	Logit
Intercept	0.0029	-0.3445
	(5.33)	(-1.83)
ρ	0.0015	1.3737
	(2.00)	(5.11)
Dum_p	0.0057	-0.1605
	(5.43)	(-0.48)
$Dum_p \times \rho$	0.0061	-0.8753
	(3.05)	(-1.38)
R^2	0.0219	0.0096

with the corresponding t-statistic in parenthesis. As seen, the signs of the coefficients are consistent with our hypothesis: the total impact of ρ given $Dum_p = 1$, i.e. the sum of β_1 and the interaction coefficient β_3, is positive and significant. To understand these results, consider the case with dummy variable $Dum_p = 1$ (i.e. when $0.5 < p < 1.5$). Here, a 0.1 increase in correlation ρ (e.g., from 0 to 0.1) increases the bubble magnitude by $\approx 0.08\%$. Also, a 0.1 unit increase in ρ increases the probability of seeing a bubble by $\approx 2.3\%$.[56]

In summary, the parameters ρ and p of the G-SVJD processes, the parameters that determine whether or not a asset price bubble exists, are highly correlated among themselves and help to explain the occurrence and the magnitude of the estimated call option bubbles. These results are particularly important because our estimation procedure does not enforce

[56]We compute the effect of a change in ρ on the predicted bubble probability in two steps. First, we calculate the average of the predicted probabilities in the original pooled data. Second, we add 0.1 to the estimated ρ and again compute the average of the predicted probabilities. The difference between the two average probabilities gives the marginal change in the probability for a small change in ρ, which is reported in the text.

any relationship between the values of the parameters p and ρ nor on the *sign* and the *magnitude* of the estimated call option bubble. In conjunction, these results provide evidence consistent with both the existence of positive asset price bubbles and the validity of the call option theory of bubbles.

6 Case Study: GameStop and Nasdaq Dot-com Bubble

In this section we apply our methodology to NDX during the dot-com bubble in the early 2000s and GameStop (GME) between 2020 and 2021. The massive run up in the prices and subsequent crash of the technology sector, i.e. the alleged *dot-com* bubble of late 1990s and early 2000s is a perfect laboratory to check whether our methodology detects a bubble. We focus on the period from early 1999 to the end of 2002, which covers the full run up and crash cycle. Similarly, GME captured the public's and policy-makers' attention in January 2021 when its price exhibited unusual fluctuations and price appreciation for reasons not related to the company's fundamentals. GME's closing price increased from $35.50 on January 15th to $347.51 on January 27th and back to $92.41 by February 3rd. As such, GME represents another opportunity to see if our methodology can identify a price bubble.[57]

For NDX, we obtain data from OptionMetrics and apply the same filters as described in Section 4. We consider the period between January 1st, 1999 and December 31st, 2002. For GME, we obtain daily options quotes from the Chicago Board Options Exchange (CBOE) DataShop. Our sample period runs from April 1st, 2020 to February 3rd, 2021. Starting with April 2020 allows us to avoid the market turmoil due to the Covid-19 crisis. This choice provides sufficient sample size for our methodology, even after accounting for the burn-in period of 180 days needed to compute the time-varying threshold used in our statistical test for detecting bubbles. The data provided by the CBOE are similar to that provided by OptionMetrics. However, the CBOE also provides option quotes at 3:45PM Eastern Time, which are generally more reliable than closing prices because they have narrower bid-ask spreads. This is particularly important for stocks like GME which are generally illiquid, increasing the likelihood that put-call parity is satisfied. Thus, we use the 3:45PM quotes

[57] News reports suggest that groups of retail traders fueled the trading activity in both GME stocks and options. Options are highly levered and if agents expect the prices to rise (fall) in the future, purchasing call (put) options is a well known strategy to benefit from such expectations. In a recent staff report (https://www.sec.gov/files/staff-report-equity-options-market-struction-conditions-early-2021.pdf) the SEC finds that both call and put options were actively traded: call options by investors who expected GME's price to keep increasing, and put option by investors who used them as an alternative say to short the stock.

and we apply an analogous data filter as described in second paragraph of section 4.[58]

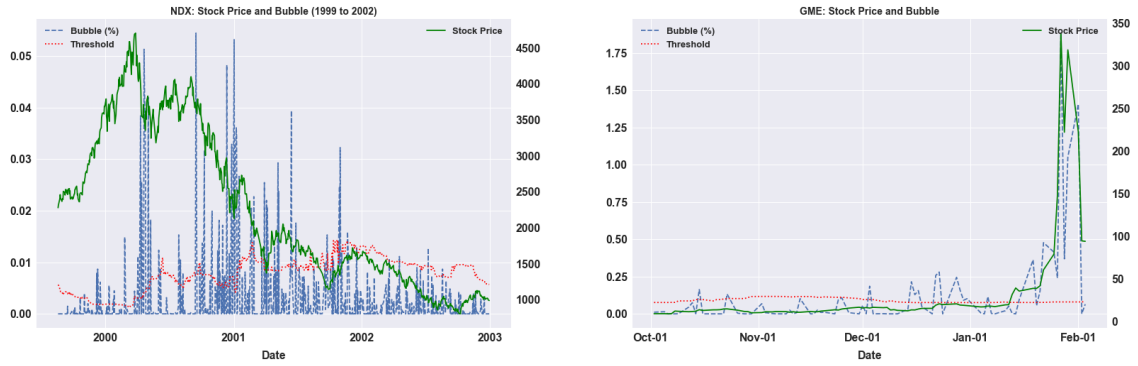

(a) NDX: Stock Price and Bubble (b) GME: Stock Price and Bubble

Figure 10: **NDX & GME: Stock Prices and Call Option Bubbles**. In both panels, the right axis shows stock prices (solid lines, green color). The left axis show estimated call option bubble magnitudes as a percentage of stock prices (dashed lines, blue color) and time-varying threshold $\mathbb{T}_t = 1.65\hat{\sigma}_t$ (dotted lines, red color).

Panel (a) of Figure 10 shows the estimated call option bubble for NDX along with the time-varying threshold (left axis) and NDX price (right axis). Our method detects a bubble in NDX starting in March 2000. The bubble persists throughout the entire year and it slowly bursts at the end of 2001. During this period the NDX price declined by more than 4500 points to around 1000 points. Beginning in 2002, the estimated call option bubbles reduce in magnitude and become insignificant.[59]

Analogous to NDX, Panel (b) of Figure 10 shows the estimation results for GME. As seen, while there are no significant bubbles in the months of October and November, there are a few instances of significant bubbles starting in mid to late December 2020. After that, as GME's price surges in the second half of January 2021, the estimated call option bubble increases almost in the same proportion. In particular, our estimates shows that a lower bound on the asset price bubble is more than 1.5% of GME's price in late January.[60] This is consistent with the extraordinary short term rise of the GME stock, daily rises in multiples of one hundred percent, from around $39 on January 20th, to $347 on January 27th, with an intra-day high in the upper $400s on January 28th. By February 3rd, GME's price dropped

[58] Also, in order to remove highly illiquid contracts we only retain put options with standardized moneyness $(= \ln(K/S)/(\sigma_{ATM}\sqrt{\tau}))$ between - 4 and 5. This additional filter only removes 2% of observations which tend to have zero volume and open interest, and unusually high implied volatilities that exceeds 500%.

[59] Even though the bubble's peak is generally identified after the bubble burst period, our approach is able to detect the ongoing/persistent bubble in NDX well before its ex-post identified peak, in real-time.

[60] In Appendix C we show that the parameters estimated from GME are compatible with a bubble ranging from 20% to 100% of the underlying asset over a one year horizon.

Table 8: **Conditional Tests**. The first row reports the percentages of days in which the null hypothesis of the statistical test (i.e. $\mathbb{B}_t = 0$) is rejected with a one-side probability of 10%. The second, third, fourth, and fifth rows report the average $RMSE_{IV}$ (i) over the entire sample period, (ii) on days when $\hat{\mathbb{B}}_t < 0$, (iii) on days when $\hat{\mathbb{B}}_t > 0$, and (iv) on days when the null is rejected, respectively.

	GME	NDX
% of days above threshold	9.98	27.71
$RMSE_{IV}(\%)$		
Entire Sample	**0.70**	**7.11**
Negative Bubbles	0.69	8.85
Positive Bubbles	0.75	6.21
Bubble Above Threshold	**0.71**	**5.28**

to \$92, which is captured by our estimated call option bubble which drops significantly by the end of the period.[61]

Finally, the formal results of the statistical test as described in Section 3.4 are shown in Table 8. The first column refers to NDX while the second column is for GME. The first row of the table reports the percentage of days with estimated positive stock price bubbles, while the lower part of the table reports the $RMSE_{IV}$ over the entire sample and sub-samples based on the signs and significance of the estimated bubbles. In the case of NDX, 10% of the days show a positive and significant bubble. Also, we notice that the average $RMSE_{IV}$ is equal to 0.70%. This is very similar to the pricing error reported in Table 3 in the case of NDX and SPX over the 2014–2018 period. Importantly, on days when we detect a bubble, the $RMSE_{IV}$ is similar to (0.71%), the average $RMSE_{IV}$ over the entire sample. In the case of GME, the average $RMSE_{IV}$ is equal to 7.11%. Although this is large when compared to the $RMSE_{IV}$ for AMZN and FB (which are around 1%), the average implied volatility of GME in our sample is 2.30, which is almost 6 times larger than those for AMZN and FB. Importantly, and consistent with the results in Table 3, on days when we detect a bubble, the $RMSE_{IV}$ is significantly lower (5.28%) than the average $RMSE_{IV}$ over the entire sample. This observation mitigates possible concerns about model misspecification. Also, the $RMSE_{IV}$ for days with negative bubbles is higher (8.25%) than

[61] Note that since NDX is an index where the bubble can also be seen as the weighted bubbles of individual stocks, its bubble magnitude will be generally smaller than those of the individual stocks. Despite this, it is interesting to observe high and persistent call option bubble magnitudes in NDX during the dot-com bubble era relative to occasional and smaller bubbles in a more recent period.

the average $RMSE_{IV}$, thus providing support for our assertion that negative bubbles are the result of noise in the option data.[62]

Summarizing, our method identifies episodes of persistent price bubbles during both the Nasdaq dot-com bubble and, more recently, during the rise and successive fall of GameStop price. Our analysis shows that our call option bubble detecting methodology can be easily implemented in real-time. Furthermore, we demonstrate that in the case of GME, options data are able to detect the onset of a bubble in mid December, when the stock price was still less than $15.

7 Conclusion

This paper presents a new approach to identifying asset price bubbles in real time using options data. We illustrate the method by applying it to the S&P 500 and Nasdaq-100 indexes and two highly liquid stocks: Amazon and Facebook between the 2014-2018 period. We also apply our methodology to the Nasaq dot-com bubble in the early 2000s and to the recent rise and fall in the price of GameStop stock. In both instances we detect large and significant bubble episodes. As such, our approach can be useful to both policy-makers and investors who need a forward-looking approach to daily, real-time monitoring of the financial system for risk-management.

[62] In the case of GME, one could be concerned that our results are influenced by specific and unusual market conditions. However, the SEC staff report (https://www.sec.gov/files/staff-report-equity-options-market-struction-conditions-early-2021.pdf) concludes that popular explanations for GME's price increase, such as a *short-squeeze* and/or a *gamma-squeeze* are not supported by the data. The SEC report concludes that the option market operated smoothly over the January–February 2021 period.

A Computational Details

The calibration discussed in section 3.2 is equivalent to solving a non-linear constrained and non-convex optimization problem (where parameters are restricted to certain bounds). Given the highly non-linear and non-convex nature of the objective function in Equation (18), we tested many optimization routines that are available in Python. We found Differential Evolution (DE), a global optimization algorithm, to be the best algorithm for our purpose. It is a derivative-free, stochastic population-based, optimization method that can search large areas of the parameter space.[63] A global optimization method is preferred to commonly used local optimizer (e.g. the widely used Nelder-Mead), as they are much less sensitive to the initial guess of the parameter values.

The accuracy and robustness of the optimization algorithm comes with a large computational cost. Despite the data filters discussed in Section 4, the estimation of the parameter vector on any single day for any of the underlying assets takes anywhere between two and 16 hours (on a system with an Intel-i7 processor at 3.60 GHz speed). We used the MARCC (Maryland Advanced Research Computing Center) system to carry out the entire estimation.[64]

B Proofs

B.1 Proof of Theorem 1

Theorem 1 (No Zero-coupon Bond Price Bubbles)**.** *Assume* $p(t, t+\tau) \leq 1$ *for all* $0 \leq t \leq t+\tau \leq T$*. Then,* $p(t,\tau) = p^*(t,\tau)$*.*

Proof. NFLVR implies $\frac{p(t,\tau)}{B_t}$ is a $\mathbb{Q}$ local martingale. $B_t \geq 0$ implies $\frac{p(t,\tau)}{B_t} \leq 1$ for all t. A bounded local martingale is a martingale. This completes the proof. □

B.2 Proof of Theorem 2

Theorem 2 (European Puts Have No Bubbles)**.** *Assume* $p(t,\tau) \leq 1$ *for all* $0 \leq t \leq t+\tau \leq T$*. Then,* $P_t^E = P_t^{E*}$

[63] See https://docs.scipy.org/doc/scipy/reference/generated/scipy.optimize.differential_evolution.html for details on Python's implementation of DE. Note that, by default, DE refines the best parameters at the end with the L-BFGS-B algorithm.

[64] See https://www.marcc.jhu.edu/about-marcc/about-us/ for details about the MARCC system.

Proof. We show P_t^E is uniformly bounded by K for all t. If not, then $P_t^E > K$ for some t. We generate a contradiction of NFLVR, by producing an arbitrage. Sell P_t^E (most one can lose is K, so this short position is bounded below). Buy $\frac{P_t^E}{\frac{p(t,\tau)}{B_t}}$ zero-coupon bonds with this cash (in units of the mma), maturing at time $t+\tau$ (this leg of the strategy is bounded below). The cost is $\frac{P_t^E}{\frac{p(t,\tau)}{B_t}}\frac{p(t,\tau)}{B_t} = P_t^E$. The strategy is admissible and self-financing since it is a buy and hold. At time $t+\tau$ the payoff is $\frac{P_t^E}{\frac{p(t,\tau)}{B_t}} - max(K - S_T, 0) > K(\frac{B_t}{p(t,\tau)} - 1) > 0$ because $P_t^E > K$. This is with probability one. Hence, an NFLVR. Contradiction.

Next, P_t^E is a supermartingale under $\mathbb{Q}$. Since it is uniformly bounded, it must be a martingale. This completes the proof. □

B.3 Proof of Theorem 3

Theorem 3 (European Calls Can Have Bubbles)**.** $C_t^E = C_t^{E*} + \delta_t(\tau)$ *where* $\delta_t(\tau) \geq 0$ *is a supermartingale with* $\delta_{t+\tau}(\tau) = 0$*. If* $\delta_t(\tau) > 0$*, then there is a bubble.*

Proof. NFLVR implies $C_t^E \geq 0$ is a $\mathbb{Q}$ local martingale. A non-negative local martingale is a supermartingale, which implies $C_t^E \geq C_t^{E*}$. Defining $\delta_t(\tau)$ as $C_t^E - C_t^{E*}$ completes the proof. □

B.4 Proof of Theorem 4

Theorem 4 (Call Bubbles and Asset Price Bubbles)**.** *Assume ND, then*

$$C_t^E = C_t^{E^*} + \beta_t - E_t\left[\beta_{t+\tau}\right]. \tag{6}$$

Or, equivalently $\delta_t(\tau) = \beta_t - E_t\left[\beta_{t+\tau}\right]$*, which is independent of* K*.*

Proof. $S_{t+\tau} - K = max(S_{t+\tau} - K, 0) - max(K - S_{t+\tau}, 0)$. Hence, $E_t\left(S_{t+\tau}\right) - Kp(t,\tau) = E_t\left(max(S_{t+\tau} - K, 0)\right) - E_t\left(max(K - S_{t+\tau}, 0\right)$, or $S_t - (\beta_t - E_t[\beta_{t+\tau}]) - Kp(t,\tau) = C_t^{E*}(\tau, K) - P_t^E(\tau, K)$, using $P_t^E = P_t^{E*}$. Note K is in units of the mma, so only $p(t,\tau)$ appears here. Put call parity is $S_t - Kp(t,\tau) = C_t^E(\tau,K) - P_t^E(\tau,K)$ Combined, this yields: $C_t^E = C_t^{E^*} + \beta_t - E_t\left[\beta_{t+\tau}\right]$. This implies $\delta_t(\tau) = \beta_t - E_t\left[\beta_{t+\tau}\right]$. This completes the proof. □

B.5 Proof of Theorem 5

Theorem 5 (Bubble Test)**.** *Consider a small time window (equal to* k *days) before time* t*. We partition the daily bubble estimates* $\{\mathbb{B}_i\}_{i=t-k,\cdots,t}$ *into two sets, and only collect observa-*

tions at times $i = t-k, ..., t$ *where* $\hat{\mathbb{B}}_i < 0$. *Call this set* Υ_-. *Let the number of elements in this set be* N_-. *For this set of observations, an unbiased estimator of* σ_t^2 *is*

$$\hat{\sigma}_t^2 = \sum_{i \in \Upsilon_-} \frac{1}{N_-} \hat{\mathbb{B}}_i^2. \tag{21}$$

Proof. The proof is based on the following lemma.

Lemma. Let x_t have mean zero, finite variance, with a symmetric and continuous distribution. Then, $Var(x_t) = E(x_t^2 \,|x_t < 0)$.

Proof of Lemma.

$Var(x_t) = E(x_t^2) = E(x_t^2 \,|x_t < 0)P(x_t < 0) + E(x_t^2 \,|x_t > 0)P(x_t > 0)$

But, by symmetry, we have that $P(x_t < 0) = P(x_t > 0) = 1/2$, and $E(x_t^2 \,|x_t < 0) = E(x_t^2 \,|x_t > 0)$. Hence, $Var(x_t) = E(x_t^2 \,|x_t < 0)$. This completes the proof of the lemma.

Given the lemma, we now prove the theorem.

Recall that $\hat{\mathbb{B}}_t = \mathbb{B}_t + \varepsilon_t$.

Under H_0 where $\mathbb{B}_t = 0$, conditioned on $t \in \Upsilon_-$.

$\sigma_{N_-}^2 = E\left[\sum_{t \in \Upsilon_-} \frac{1}{N_-} \hat{\mathbb{B}}_t^2 \mid t \in \Upsilon_-\right]$

$= E\left[\sum_{t \in \Upsilon_-} \frac{1}{N_-} \varepsilon_t^2 \mid t \in \Upsilon_-\right]$

$= \sum_{t \in \Upsilon_-} \frac{1}{N_-} E\left[\varepsilon_t^2 \,|\varepsilon_t < 0\right]$

This last inequality follows because the errors are independent.

By the lemma, letting $x_t = \varepsilon_t$, we have

$E\left[\varepsilon_t^2 \,|\varepsilon_t < 0\right] = \sigma_t^2$.

Substitution yields

$= \sum_{t \in \Upsilon_-} \frac{1}{N_-} \sigma_t^2$, which completes the proof.

C Simulation Exercise

In this section we study how the size of the estimated bubble depends on (1) the time-to-maturity of the options and (2) the value of the parameters p and ρ in the G-SVJD model.

Regarding the first point, Figure 2 depicts the intuitive idea that the size of the detected bubble increase as the maturity of the options increase and, hypothetically, if we could observe options with time-to-maturity equal to T (the terminal time) the option market would be able to fully reveal the size of the bubble in the underlying asset. However, (i) T is conceptually quite large (as it corresponds to the end of the economy) and (ii) most of the liquidity in the option market is concentrated on short-medium maturity options (in our

empirical exercise we focus on options with maturity between 7 and 50 calendar days). The higher liquidity of short maturity options makes our inference more robust, but, at the same time, it also implies that our estimates represents a lower bound for the magnitude of the bubble in the underlying asset.

Regarding the second point, within the lenses of the G-SVJD model, two parameters (ρ and p) jointly determine whether the underlying asset is a martingale or strict supermartingale (see Section 3.1). The sections aims at determining how the above two parameters impact the size of the estimated bubble. We perform a simulation study using the G-SVJD model. We take the parameters from the estimation results on the GME stock. In particular, we take the median of the estimated parameters on the days when the bubble magnitude is higher than the threshold level $\mathbb{T}_t$ as seen in Figure 10.[65] We then consider a set of parameters ρ and p that make the G-SVJD process a martingale (which implies the absence of a bubble) or a supermartingale (which implies the presence of a bubble), as discussed in Section 2.1. For the no-bubble case we fix $\rho = -0.90$ and $p = 0.3$, while for the bubble case we consider all the combinations between $\rho \in \{0.1, 0.5, 0.9\}$ and $p \in \{0.6, 1, 1.4\}$, for a total of nine parameter combinations. Finally, we normalize the initial stock price to be $S_0 = 100$, and we set the risk-free rate and dividend yield to zero.

For each parameter vector we simulate $N = 10,000,000$ trajectories over a 1-year horizon (i.e. 360 days) using a daily frequency. For each maturity τ ($\tau = 1, \cdots, 360$), we:

- compute the price of a set (N_K) of put options with strike prices $K \in \{90, 95, 100, 105, 110\}$ as $P_{\tau,K} = \frac{1}{N}\sum_{n=1}^{N} \max(K - S_{\tau,n}, 0)$. Recall that, as described in Section 2, put options are not affected by a bubble in the underlying asset.

- Using the price of the underlying asset (S_0) and the put prices from above, we compute the market price of the corresponding call options ($C_{\tau,K}$) via put-call parity. In this case, if the underlying asset is affected by a bubble, the resulting call price would be affected by it as well.

- Then, we compute the fundamental price of the call options as $C^*_{\tau,K} = \frac{1}{N}\sum_{n=1}^{N} \max(S_{\tau,n} - K, 0)$.

- Finally, the bubble magnitude is given by $B_\tau = \frac{1}{N_K}\sum_{j=1}^{N_K}\left(C_{\tau,K_j} - C^*_{\tau,K_j}\right)$.[66]

[65] The parameters are: $V_0 = 8.65$, $\bar{\nu} = 13.86$, $\kappa = 5$, $\sigma_v = 4.57$, $\mu_y = -0.79$, $\sigma_y = 0.87$, $\lambda = 0.93$.

[66] Alternatively, one can compute the size of the bubble, for a given horizon τ, as the difference between the price of the underlying asset and its fundamental value which we can computed as $FV_\tau = \frac{1}{N}\sum_{n=1}^{N} S_{\tau,n}$. Although such a computation is only feasible in a simulation setting we confirm that both approaches leads to identical results.

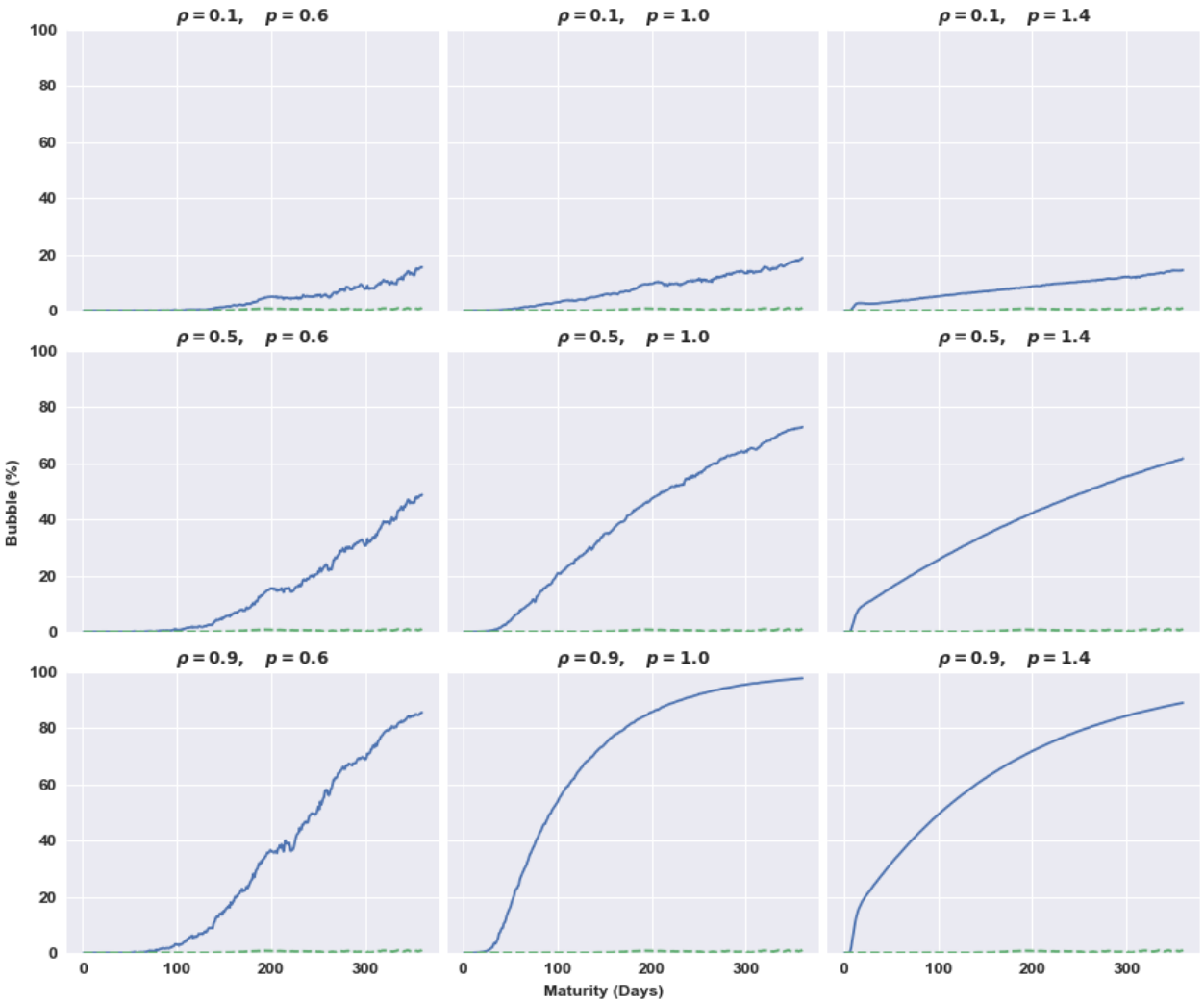

Figure 11: **Bubble's magnitude as a function of the option's time-to-maturity**: The x-axis shows the option maturity (in days) while y-axis shows the bubble magnitude (%). The blue solid-line corresponds to the case in which the parameters ρ and p are in the bubble range. (see shaded area in Figure 3).The green dotted-line shows the bubble magnitude (expected to be zero) when the above parameter are in the no-bubble region.

The blue solid line in Figure 11 reports the results of the numerical exercise for the nine different parameter combinations. Regardless of the parameter combination, the bubble magnitude (B_τ) increases with the maturity of the options. While both parameters ρ and p affect the size and the trajectory of the estimated bubble, the figure seems to indicate that ρ has the largest effect on the bubble size. Importantly, Figure 11 shows that even a modest bubble over a short horizons, can be the reflection of a much larger bubble over longer horizons. Moreover, the simulation study confirms that the size of the bubble is independent of the strike price K. As a benchmark, the green line in Figure 11 shows the results for the

no-bubble parameters.

As a further graphical illustration, Figure 12 highlights the effect of a bubble on puts' and calls' implied volatilities. The figure shows that (i) the implied volatility computed using put options (blue solid line) is always equal to the implied volatility computed using call prices obtained via put-call parity (red dots); (ii) in the presence of a bubble the implied volatility computed on call prices obtained via risk-neutral pricing (dotted black line) is consistently lower (thus, the price of those call options will be lower as well); and (iii) the gap between the IV curves (and, as a consequence, the magnitude of the bubble,) grows with the time to maturity of the options.

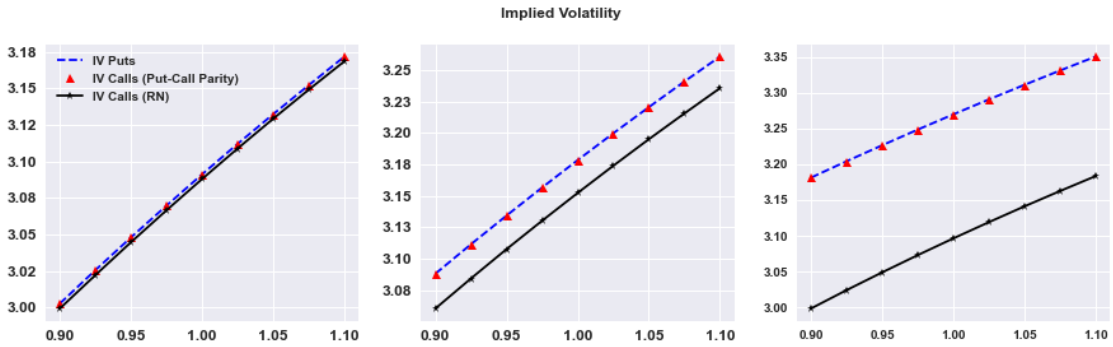

Figure 12: **Bubble and options implied volatility**: The three panels show the implied volatility according to the G-SVJ model with parameters $V_0 = 8.65$, $\bar{\nu} = 13.86$, $\kappa = 5$, $\sigma_v = 4.57$, $\mu_y = -0.79$, $\sigma_y = 0.87$, $\lambda = 0.93$. $\rho = 0.9$ and $p = 1$ are chosen to make the G-SVJ model a supermartingale (i.e. in the bubble region). The left, middle, and right panels correspond to options with time-to-maturity of 10, 20 and 30 days, respectively. In each panel, the solid (blue) lines show the implied volatility computed from put prices, the (red) dots show the implied volatility computed from call prices obtained via put-call parity, and the dotted (black) lines shows the implied volatility computed from call prices obtained via risk-neutral pricing.

References

Andersen, L. and V. Piterbarg (2007). Moment Explosions in Stochastic Volatility Models. *Finance and Stochastics 11*, 29–50. 1, 3.1, 28

Andersen, T. G., O. Bondarenko, and M. T. Gonzalez-Perez (2015). Exploring Return Dynamics via Corridor Implied Volatility. *The Review of Financial Studies 28*(10), 2902–2945. 4

Andersen, T. G., N. Fusari, and V. Todorov (2015). Parametric Inference and Dynamic State Recovery from Option Panels. *Econometrica 83*, 1081–1145. 1, 3.1, 34, 5.1, 43

Andersen, T. G., N. Fusari, and V. Todorov (2017). Short-term market risks implied by weekly options. *The Journal of Finance 72*(3), 1335–1386. 1, 3.2, 4, 5.1

Andersen, T. G., N. Fusari, V. Todorov, and R. T. Varneskov (2019). Unified Inference for Nonlinear Factor Models from Panels with Fixed and Large Time Span. *Journal of Econometrics, forthcoming 212*, 4–25. 34

Bandi, F., N. Fusari, and R. Reno' (2021). Structural Stochastic Volatility. working paper. 1

Bates, D. S. (1996). Jumps and Stochastic Volatility: Exchange Rate Processes Implicit in Deutsche Mark Options. *Review of Financial Studies 9*, 69–107. 1, 3.1, 3.1, 29

Black, F. and M. Scholes (1973). The pricing of options and corporate liabilities. *Journal of political economy 81*(3), 637–654. 3

Büchner, M. and B. Kelly (2022). A factor model for option returns. *Journal of Financial Economics 143*(3), 1140–1161. 1

Cao, J. and B. Han (2013). Cross section of option returns and idiosyncratic stock volatility. *Journal of Financial Economics 108*(1), 231–249. 1

Carr, P. and L. Wu (2003). What Type of Process Underlies Options? A Simple Robust Test. *Journal of Finance 58*, 2581–2610. 1

Chabi-Yo, F., C. Dim, and G. Vilkov (2021). Generalized Bounds on the Conditional Expected Excess Return on Individual Stocks . *Management Science (forthcoming)*. 1

Christoffersen, P., M. Fournier, and K. Jacobs (2018, 02). The factor structure in equity options. *Review of Financial Studies 31*, 595–637. 1

Christoffersen, P. and K. Jacobs (2004). The Importance of the Loss Function in Option Valuation. *Journal of Financial Economics 72*, 291–318. 3.2

Cox, A. and D. Hobson (2005). Local Martingales, Bubbles and Option Prices. *Finance and Stochastics 9*, 477–492. 1, 2

Delbaen, F. and H. Shirakawa (2002). No Arbitrage Condition for Positive Diffusion Price Processes. *Asia-Pacific Financial Markets 9*, 159–68. 2.1, 51

Duffie, D., J. Pan, and K. Singleton (2000). Transform Analysis and Asset Pricing for Affine Jump-Diffusions. *Econometrica 68*, 1343–1376. 1, 3.1

Giglio, S., M. Maggiori, and J. Stroebel (2016). No-bubble condition: Model-free tests in housing markets. *Econometrica 84*, 1047–1091. 12

Goyal, A. and A. Saretto (2009). Cross-section of option returns and volatility. *Journal of Financial Economics 94* (2), 310–326. 1

Harrison, M. and D. Kreps (1978). Speculative Investor Behavior in a Stock-Market with Heterogeneous Expectations. *Quarterly Journal of Economics 92*, 323–336. 1

Herdegen, M. and M. Schweizer (2016). Strong bubbles and strict local martingales. *International Journal of Theoretical and Applied Finance 19*. 19

Heston, S., M. Loewenstein, and G. Willard (2007). Options and Bubbles. *Review of Financial Studies 20*, 359–390. 1, 2, 19

Heston, S. L. (1993). A closed-form solution for options with stochastic volatility with applications to bond and currency options. *The review of financial studies 6* (2), 327–343. 1, 3.1, 29

Jacod, J. and P. Protter (2010). Risk Neutral Compatibility with Option Prices. *Finance and Stochastics 14*, 285–315. 18

Jarrow, R. (2015). Asset price bubbles. *Review of Financial Economics 7*, 201–218. 1, 1, 2, 2.1, 2.1

Jarrow, R. (2016). Asset price bubbles and the land of oz. *The Journal of Portfolio Theory Winter*, 1–6. 11

Jarrow, R. (2021). *Continuous-Time Asset Pricing Theory: A Martingale-Based Approach. 2nd ed.* Springer. 2.1, 16, 19, 2.1, 22, 3.2

Jarrow, R. and S. Kwok (2020). Inferring financial bubbles from option data. Working paper, Cornell University. 1

Jarrow, R. and S. Lamichhane (2021). Asset price bubbles, market liquidity, and systemic risk. *Mathematics and Financial Economics 15*, 5–40. 38

Jarrow, R., P. Protter, and J. San Martin (2020). Asset price bubbles: An invariance theorem. Working paper, Cornell University. 2.1, 3.1

Jarrow, R., P. Protter, and K. Shimbo (2010). Asset Price Bubbles in Incomplete Markets. *Mathematical Finance 20*, 145–185. 1, 1, 1, 2, 22

Lions, P. and M. Musiela (2007). Correlations and bounds for stochastic volatility models. *Annales de l'Institut Henri Poincare (C) Non Linear Analysis 24*, 1–16. 3.1

Loewenstein, M. and G. Willard (2000a). Local martingales, arbitrage and viability: free snacks and cheap thrills. *Economic Theory 16*, 135–161. 1, 2

Loewenstein, M. and G. Willard (2000b). Rational equilibrium asset pricing bubbles in continuous trading models. *Journal of Economic Theory 91*, 17–58. 1, 2

Loewenstein, M. and G. Willard (2013). Consumption and bubbles. *Journal of Economic Theory 148*, 563–600. 19

Medvedev, A. and O. Scaillet (2007). Approximation and calibration of short-term implied volatilities under jump-diffusion stochastic volatility. *Review of Financial Studies 20*, 427–459. 1

Merton, R. (1973). Theory of rational option pricing. *Bell Journal of Economics 4*, 141–183. 2.2.2

Merton, R. (1976). Option Pricing when Underlying Asset Returns are Discontinuous. *Journal of Financial Economics 3*, 125–144. 1, 3.1, 3.1, 29

Phillips, P. C. B. and S. Shi (2018). Real time monitoring of asset markets: Bubbles and crises. Cowles Foundation Discussion Paper 2152, Yale University. 1

Phillips, P. C. B., S. Shi, and J. Yu (2015a). Testing for multiple bubbles: Historical episodes of exuberance and collapse in the s&p 500. *International Economic Review 56*, 1043–1078. 1

Phillips, P. C. B., S. Shi, and J. Yu (2015b). Testing for multiple bubbles: Limit theory of real-time detectors. *International Economic Review 56*, 1079–1134. 1

Scheinkman, J. (2013). Speculation, trading and bubbles. Working Paper 050, Princeton University. 1

Todorov, V. (2019). Nonparametric spot volatility from options. *Annals of Applied Probability 29*, 3590–3636. 1

Xiong, W. (2013). Bubbles, crises, and heterogeneousbeliefs. NBER Working Paper 18905, NBER. 1

Zhan, X., B. Han, J. Cao, and Q. Tong (2021, 06). Option Return Predictability. *The Review of Financial Studies*. 1